Search for New Physics in the Same Sign Dilepton final state with b Jets and Missing Energy at the LHC

D. Barge, C. Campagnari, D. Kovalskyi, V. Krutelyov

University of California, Santa Barbara

W. Andrews, G. Cerati, D. Evans, F. Golf, I. MacNeill, S. Padhi, Y. Tu, F. Würthwein, A. Yagil, J. Yoo

University of California, San Diego

L. Bauerdick, K. Burkett, I. Fisk, Y. Gao, O. Gutsche, B. Hooberman, S. Jindariani, J. Linacre, V. Martinez Outschoorn

Fermi National Accelerator Laboratory, Batavia, Illinois

Abstract

A search for New Physics in the same sign dilepton final state with at least two b jets and $\not{E}_T$ is performed. This analysis uses a data sample collected with the CMS detector of pp collisions at a centre-of-mass energy of 7 TeV, corresponding to an integrated luminosity of $4.68\ \mathrm{fb}^{-1}$. For these searches, the dominant background is from $t\bar{t}$ events. No excess above the standard model background expectation is observed. Upper limits at 95% confidence level are set on the number of observed events.

1 Introduction

The CMS Collaboration recently published a search for new physics in same-sign top production using events with same-sign isolated dileptons, jets, and $\not{E}_T$ [1]. In that study, as well as a closely related one [2, 3, 4] the major background is from $t\bar{t}$ production, as shown in Fig. 1.
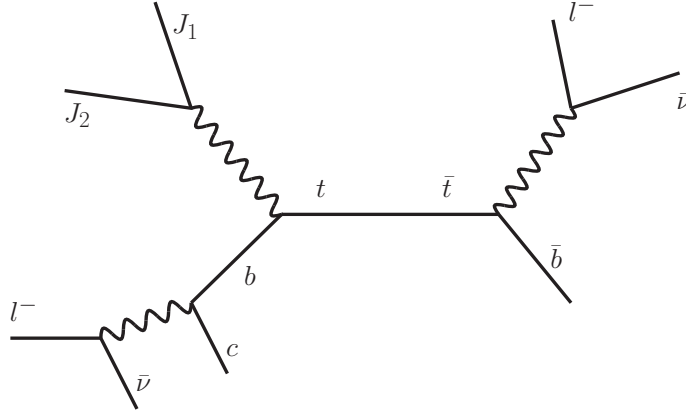

Figure 1: Diagram for $t\bar{t}$ decays giving rise to same-sign dilepton final states

The dominant source of same-sign dileptons in $t\bar{t}$ events are produced via, $t \to Wb$; where one of the leptons is from $W \to \ell\nu$ and the other originates from semi-leptonic b decays. We refer to the first as "real lepton" and the second as "fake lepton". An additional requirement on the number of b jets ≥ 2, is expected to reduce this background significantly as a b-quark can not produce an isolated lepton and at the same time provide a b-tag.

Same-sign dileptons in association with two or more b-quarks appear naturally in many new physics scenarios. They have been proposed as signatures of supersymmetry (SUSY) where heavy flavor (top or bottom) jets appear naturally [16, 17, 18, 19], in particular in processes with virtual stop contributions [20, 21], those with resonant stop [22], all alternatively described with simplified models (SMS) [23]; color-octet scalar production (either as sgluons in the context of SUSY [24], or non-SUSY in the context of minimal flavor violation [25]); models of maximal flavor violation [26, 27, 28]; same-sign top quark production from flavor changing neutral currents in the top sector [33]; pair production of $T_{5/3}$ [29]; and top compositeness [30, 31, 32] among others.

All of these new physics scenarios have in common that the isolated same-sign leptons are typically decay products of on-shell W's, thus allowing us to increase the minimum lepton p_T requirements in our search to 20 GeV, which reduces backgrounds even further. The combination of requiring at least two b jets and increasing the lepton p_T threshold to 20 GeV reduces the standard model backgrounds by roughly a factor 20 over a more generic search [2, 4].

For the purpose of this note we restrict ourselves to the ee, $e\mu$, and $\mu\mu$ final states, *i.e.*, we do not consider τ's, except in the case that the τ decays leptonically.

This note is organized as follows. A brief description of the event baseline selections is given in Section 2, followed by the definitions of the signal search regions in Section **??**. Estimates of efficiencies for leptons, $\not{E}_T$, H_T, and b-tags, components of the event selection, are given in Section 3. We then describe methods to predict background contributions in Section 4, including predictions from simulation and from data, detailed in Section 5. Results of background predictions for the defined search regions are compared with observed events in data in Section 7, supported by an exclusive (disjoint) breakdown of contributions in Appendix A. Comparisons of the predicted and observed events, together with inputs relevant to signal selection systematic uncertainties described in Section 6, are then used to interpret our findings as upper limits on production of signal events beyond the background predictions 8 and also interpret them as constraints on parameters of various new physics scenarios, as provided in Section 9.

2 Baseline Event Selection

This analysis is based on the same-sign dilepton search documented in AN-2011/468 [3] and corresponds to an integrated luminosity of 4.68 fb^{-1}. In that study we searched for events with two isolated same-sign leptons in association with 2 additional jets and $\not{E}_T$. Here we re-use most of the baseline event selection as summarized

1

below. In addition, we require at least 2 b-tagged jets using Simple Secondary Vertex High Efficiency Medium (SSVHEM) working point tagger. This tagger relies on reconstructed secondary vertices with at least two tracks and an IP significance of at least 3.3 and provides a b-jet tagging efficiency of about 60% with a roughly 5% (15%) systematic uncertainty for jet $p_T < 240(> 240)$ GeV and a tagging rate of light flavor jets in the 2–5% range, increasing with the jet momentum [5].

We thus discuss here only differences and briefly summarize the basic kinematics and triggers. For more details, we refer to [3].

- Events have to pass one of the dilepton triggers without an HT requirement.

- There should be at least two isolated same-sign leptons (ee, $e\mu$, and $\mu\mu$) with $|\eta| < 2.4$.

- We require both leptons to have $p_T >20$ GeV.

- We tighten the isolation cut on the leptons to 0.1.

- At least two particle flow jets tagged using SSVHEM tagger with $p_T > 40$ GeV and $|\eta| < 2.4$ corrected with L1FastL2L3 corrections.

- The selected jets must be separated from the leptons by $\Delta R > 0.4$.

- $\not{E}_T > 30$ GeV.

- We remove dilepton events with invariant mass $M_{ll} < 8$ GeV.

- We veto events if a third lepton is satisfying the following:

    - (an electron) passes $|\eta| < 2.5$, and a loosened identification, similar to WP90 ID-only and the `CaloIdT_TrkIdVL` trigger requirements: $h/e < 0.1(0.075)$, $|\delta\eta_{\text{in}}| < 0.007(0.009)$, $|\delta\phi_{\text{in}}| < 0.15(0.10)$, and $\sigma_{i_\eta i_\eta} < 0.01(0.03)$ in EB (EE);

    - (for a muon) passes all identification requirements of the signal selection except for the calorimeter veto requirements;

    - has relative isolation < 0.2;

    - makes an opposite-sign same-flavor pair with either of the hypothesis leptons such that the pair has a mass within 15 GeV of the Z mass.

3 Selection Efficiency

3.1 Data - Monte Carlo Scale Factor for Leptons

The efficiencies of the lepton isolation and identification requirements (including all quality requirements) are measured with the tag&probe method in dilepton Z events using the full 2011 dataset. The efficiency of the identification requirements is a property of the lepton itself and is directly applicable to the leptons in signal events. The efficiency of the isolation requirement, however, is a strong function of all other (mainly hadronic) activity in the event. The following results are based on measurements using the full dataset and compared to simulation that is re-weighed to have a pile-up distribution comparable to that observed in data.

The electron selection efficiencies are measured in events passing the `Ele17..._SC8_Mass30` and `Ele17.._Ele8_Mass30` triggers, which require one well-identified electron and one super-cluster or GSF electron with $p_T > 8$ GeV forming a pair with a mass above $30 \, \text{GeV}/c^2$. For higher p_T electrons, the `Ele32...SC_17` triggers are also used, which require one well identified electron and one super-cluster with $p_T > 17$ GeV. In the tag&probe analysis the electron tag is required to match to the well-identified electron from the trigger and also to pass all the electron requirements described in [3]. The probe electron is required to have

- $p_T > 20$ GeV, $|\eta| < 2.4$, excluding the superclusters with $1.4442 < |\eta| < 1.566$.

The isolation efficiency is measured with the probes passing all electron selections , except for the trigger requirement and the isolation itself. The identification efficiency is measured with probes passing the isolation requirement. Results of the measurement are summarized in Table 1. The contribution from the Z events is based

on simple counting in the mass range of 86–96 GeV/c, the MC contribution includes Wjet events to match the expected residual backgrounds in this mass window. The following sources of systematic uncertainty are attributed to this measurement: background contribution, selection of dielectron events, factorization of the isolation and ID parts. The size of the background contribution can be estimated using MC alone and also tested in data with the same-sign dielectron events, which should represent the number of backgrounds reasonably well. The effect of backgrounds on the measured efficiency is established to be approximately 2% for the combined identification and isolation selection efficiency. The narrow mass window used to count electron pairs introduces a bias of about 3% to the measured efficiency by rejecting failing probes that happen to have a worse resolution or a shift in the measured momentum. This bias is expected to approximately cancel in data and simulation. We include a half of the 3% as a source of systematics. Based on simulation alone, the combined selection efficiency, measured with respect to the probe electron, differs from the product of the components by approximately 1% or less depending on the momentum range. All of these effects combined give a systematic uncertainty on the total data-to-MC scale factor in the lepton selection efficiencies of 2.5% for $p_T > 20$ GeV.

		20 - 40 GeV	40 GeV -
	MC	0.9268 ± 0.0004	0.9768 ± 0.0002
ISO	DATA	0.9247 ± 0.0003	0.9737 ± 0.0002
	DATA/MC	0.9977 ± 0.0005	0.9968 ± 0.0003
	MC	0.8069 ± 0.0005	0.8500 ± 0.0004
ID	DATA	0.8005 ± 0.0005	0.8343 ± 0.0004
	DATA/MC	0.9921 ± 0.0008	0.9815 ± 0.0006
	MC	0.7478 ± 0.0005	0.8303 ± 0.0004
ID X ISO	DATA	0.7403 ± 0.0005	0.8124 ± 0.0004
	DATA/MC	0.9899 ± 0.0010	0.9784 ± 0.0007

Table 1: Electron isolation and identification efficiencies measured with the tag&probe method. The uncertainties are statistical only.

The muon selection efficiencies are measured using events passing the double-muon trigger. The tag muon is required to pass all of the muon selection requirements described in [3]. The probe muon is required to pass

- $p_T > 20$ GeV/c;

- $|\eta| < 2.4$;

- have both the global and the tracker muon types.

Both the isolation and the identification efficiency are measured using probes failing only the requirement in question, assuming the efficiencies factorize. Results of the muon identification and isolation efficiency measurements are presented in Table 2. As expected, the identification efficiency for muons measured in data and in MC agree well, while there is some discrepancy for the isolation efficiency. Similar sources of systematic uncertainty are considered here as those considered for electrons. Most of the reconstructed (probe) muons are real muons and the measurement of the identification efficiency is not affected significantly by backgrounds. With the tighter mass window used here to select events, the backgrounds are estimated to be small. This narrow mass window, however, introduces a bias of about 1.5% to the measured efficiency by rejecting failing probes that happen to have a worse resolution or a shift in the measured momentum. This bias is expected to approximately cancel in data and simulation. We include a half of the 1.5% as a source of systematics. We assign a systematic uncertainty of 1% on the identification and isolation efficiency measurement from a comparison between the simple counting of Z events and fitting the mass shape to a gaussian signal and an exponential background component. Based on studies in MC events, we find that the isolation and the identification efficiencies factorize near-perfectly and do not assign any additional systematic uncertainty. The total systematic uncertainty on the muon efficiency measurement in data, simply covering the full momentum range, is 2%.

The tag&probe results in Tables 1 and 2 show that for leptons with $p_T > 20$ GeV used in this analysis both the ID part and the isolation parts of the lepton selection are reproduced well by simulation, already within the systematic uncertainties quoted above. Application of this measurement based on Z events to the signal events incurs an additional uncertainty due to potential mismodeling of the isolation requirement. In agreement with Ref. [3], we assign a systematic uncertainty of 5% due to modeling of the isolation efficiency for signal events. Considering the small size of the difference between data and simulation reported in Tables 1 and 2, compared to the systematic

		20 - 40 GeV	40 GeV -
ISO	MC	0.9111 ± 0.0003	0.9747 ± 0.0002
	DATA	0.8969 ± 0.0003	0.9668 ± 0.0002
	DATA/MC	0.9844 ± 0.0004	0.9919 ± 0.0002
ID	MC	0.9710 ± 0.0002	0.9612 ± 0.0002
	DATA	0.9666 ± 0.0002	0.9561 ± 0.0002
	DATA/MC	0.9955 ± 0.0003	0.9947 ± 0.0003
ID X ISO	MC	0.8847 ± 0.0003	0.9369 ± 0.0002
	DATA	0.8669 ± 0.0003	0.9244 ± 0.0002
	DATA/MC	0.9799 ± 0.0005	0.9866 ± 0.0003

Table 2: Muon isolation and identification efficiencies measured with the tag&probe method. The uncertainties are statistical only.

uncertainty applicable to the analysis, we approximate the scale factor to be 1.0 for both simulated signal and backgrounds and propagate the uncertainty described above to the relevant part of the analysis (signal selections) described in Section 6.

3.2 Data - Monte Carlo Scale Factor for b-jets

We apply an average scale factor of 0.96 measured using $t\bar{t}$ events for the SSVHEM tagger [34]. The uncertainty on the scale factor is 5 (15)% for jets with $p_T < 240(> 240)$ GeV, as recommended by the b-tagging POG [35] and apply it to the analysis as described in Section 6.

4 Background Contributions

We are following the same strategy in estimating the background contributions. Contributions with genuine same-sign isolated lepton pairs are estimated from simulation, while the contributions from leptons arising from jets (fakes) and from genuine opposite-sign pairs with a lepton charge misreconstruction (charge flips) are measured in data using control data samples. The data-driven estimates are described in the next section. In addition, as a reference, we are using all relevant available simulated samples to get a feeling of the expected yields from simulation alone. As will be shown later in Section 7, contributions with genuine same-sign isolated dileptons are comparable to those estimated from events with fake leptons, while the predictions from charge flips are relatively low. These findings are in a fair agreement with direct estimates from simulation.

We use MC to estimate contributions from the following SM production processes with genuine same-sign isolated dileptons:

- $qqW^{\pm}W^{\pm}, WWW, WWZ, WZZ, ZZZ, WW\gamma, t\bar{t}W, t\bar{t}Z, t\bar{t}\gamma$ and double parton $W^{\pm}W^{\pm}$ with two real leptons in the final state.

- $WZ, W\gamma^{\star}$ (0.25 GeV $< m_{\gamma^{\star}} < 12$ GeV), and ZZ with two real leptons in the final state.

- $W\gamma$ with one real lepton and a photon conversion. This background is a priori not estimated by the fake rate method because the photon is generally isolated.

Details on the sameples used and the corresponding cross sections can be found in Ref. [3].

5 Data Driven Background Estimation Methods

We have developed two data-driven methods to estimate the two potentially dominant backgrounds. The first method provides an estimate of the number of events with fake leptons (jets misidentified as leptons). The second method is used to estimate the number of genuine leptons reconstructed with an incorrect charge sign.

5.1 Data Driven prediction for fake lepton backgrounds

We predict the background from fake leptons using the technique previously implemented in 2010 data analysis and documented in [6]. The idea is to count the number of events for which one lepton passes all final selections

and a second lepton fails the nominal requirements but passes a looser set of requirements. We refer to the former lepton as a "numerator" lepton (n), and the latter a "non-numerator" (denominator and not numerator, or $\bar{n}$). The denominator objects are also referred to as fakeable objects (FO). The ratio of "numerator" to "denominator" objects is called a "fake rate", FR (also known as tight-to-loose ratio, TL). A fake rate function is measured in an independent data sample of multijet events. This fake rate function is measured in bins of lepton p_T and $|\eta|$, separately for electrons and muons.

The numerator selections are detailed in Section 2. The denominator selections are exactly the same as in the inclusive analysis [3]. They are listed below for completeness.

Muon denominator definition is to relax the following muon requirements from Section **??**:

- χ^2/ndof of global fit < 50 (was < 10);

- transverse impact parameter with respect to the selected vertex is < 2 mm (was < 200 μm);

- Iso is set to be $Iso < 0.4$ (was < 0.1).

Electron denominator definition is to relax the following electron requirements from Section **??**:

- the impact parameter cut is removed (was < 200 μm);

- Iso is set to be $Iso < 0.6$ (was < 0.10).

We thus use an extrapolation in isolation (and impact parameter) to estimate the fake lepton backgrounds in both electrons and muons. This choice of the denominator is designed to be safe determining contributions from all types of fake lepton candidates arising from jets. It has already been extensively tested in the inclusive (pre-tagged) same-sign dilepton analysis [3], where the fake-isolated leptons are expected to be dominated by heavy flavor jets, in which the lepton candidate is predominantly a real lepton from b/c-quark semileptonic decays. In this analysis, as discussed in detail below, we find that isolated lepton candidates not arising from heavy flavor decays have a much larger fraction (dominant for electrons) of all fake leptons. Closure tests performed on $t\bar{t}$ simulation (still expected to be the dominant source of fakes) confirm this choice of denominator definition works here as well.

Samples of multijet (inclusive QCD) events in data are selected among events with a single lepton trigger present. The same requirements are applied to select the multijet-dominated events as in the inclusive analysis [3].

We repeat all relevant studies performed with 2011 data, as documented in Ref. [3]. These include

- extraction of the fake rates in simulation and data;

- measurement of the fake-rate dependence on the *opposite-side* jet p_T, as a measure of the dependence on the progenitor parton momentum in data;

- closure tests on $t\bar{t}$ after the baseline and search region selections.

Results of other tests performed in Refs. [3, 6] apply here in part, with the main caveat that they are the most relevant for fakes not from the heavy flavor as well:

- closure tests in W+jets and double-fake in QCD MC samples (even though none of these are expected to contribute significantly even at the baseline selection level);

- estimates of the residual W+jet and Z contamination in the sample;

- comparison with the fake rate measured in events with enhanced heavy flavor contribution using b-tagging (the variation observed here is up to about 20% for electrons and muons in both simulation and data and are fractionally much less important here).

We arrive to essentially the same conclusions on the performance of the fake-rate method as we did in the past. In particular, we find that the method works reasonably well, still with a systematic uncertainty of about 50%. In the following we summarize the measurement of the fake rate and provide several highlights of the studies with the current dataset.

The nominal fake rates are measured requiring an "opposite side" jet with $p_T > 40$ GeV, separated by $\Delta R > 1.0$ from the FO. The electron fake rates are measured separately for triggers with an isolation requirement and for triggers without any isolation requirement on the electron. Results of the measurement are summarized in Table 3 for triggers with calorimeter isolation (as used for $e\mu$ events), and in Table 4 for triggers with both the calorimeter and tracker isolation requirements (as used for ee events). Results for electron triggers without an isolation requirement are provided in Table 5 as a reference. The muon fake rates are measured using all single-muon triggers described in Ref. [3]. The measurement is summarized in Table 6.

p_T \\ $|\eta|$	10.000 – 15.000	15.000 – 20.000	20.000 – 25.000	25.000 – 35.000	35.000 – 55.000
0.000 – 1.000	0.2773 ± 0.0072	0.1784 ± 0.0072	0.1759 ± 0.0079	0.1789 ± 0.0084	0.2583 ± 0.0148
1.000 – 1.479	0.2749 ± 0.0121	0.2177 ± 0.0132	0.1977 ± 0.0115	0.1924 ± 0.0117	0.3026 ± 0.0197
1.479 – 2.000	0.2415 ± 0.0152	0.1806 ± 0.0137	0.1871 ± 0.0099	0.1916 ± 0.0095	0.2379 ± 0.0135
2.000 – 2.500	0.2827 ± 0.0146	0.2607 ± 0.0156	0.2420 ± 0.0119	0.2561 ± 0.0116	0.3225 ± 0.0154

Table 3: Electron fake rate measured in bins of the electron candidate p_T and η for electrons collected using triggers with a calorimeter isolation requirement.

p_T \\ $|\eta|$	10.000 – 15.000	15.000 – 20.000	20.000 – 25.000	25.000 – 35.000	35.000 – 55.000
0.000 – 1.000	0.3783 ± 0.0218	0.2932 ± 0.0279	0.2365 ± 0.0298	0.2713 ± 0.0324	0.3690 ± 0.0527
1.000 – 1.479	0.3556 ± 0.0357	0.3617 ± 0.0496	0.2364 ± 0.0405	0.2353 ± 0.0460	0.4667 ± 0.0644
1.479 – 2.000	0.2326 ± 0.0372	0.1638 ± 0.0344	0.2000 ± 0.0332	0.2260 ± 0.0314	0.2793 ± 0.0426
2.000 – 2.500	0.3357 ± 0.0399	0.2736 ± 0.0433	0.2362 ± 0.0377	0.2681 ± 0.0377	0.3645 ± 0.0465

Table 4: Electron fake rate measured in bins of the electron candidate p_T and η for electrons collected using triggers with calorimeter and tracker isolation requirements.

p_T \\ $|\eta|$	10.000 – 15.000	15.000 – 20.000	20.000 – 25.000	25.000 – 35.000	35.000 – 55.000
0.000 – 1.000	0.1985 ± 0.0141	0.1535 ± 0.0177	0.1260 ± 0.0212	0.1567 ± 0.0247	0.2198 ± 0.0434
1.000 – 1.479	0.1951 ± 0.0253	0.1867 ± 0.0318	0.1870 ± 0.0352	0.1800 ± 0.0384	0.3333 ± 0.0624
1.479 – 2.000	0.1880 ± 0.0339	0.1696 ± 0.0355	0.1481 ± 0.0279	0.1548 ± 0.0279	0.2596 ± 0.0430
2.000 – 2.500	0.2583 ± 0.0356	0.3084 ± 0.0446	0.1797 ± 0.0339	0.2836 ± 0.0389	0.3191 ± 0.0481

Table 5: Electron fake rate measured in bins of the electron candidate p_T and η for electrons collected using triggers without isolation requirements.

Figures 2 and 3 show the projection on p_T and $|\eta|$ of these fake rates for electrons and muons, respectively. Electron fake rates measured for triggers with an isolation requirement are slightly higher than those for triggers without an isolation requirement, as expected. The difference, even though it's not very large, is significant enough and we treat fake rates for these triggers separately. The dependence of the fake rates on the away-jet momentum is also shown on these figures.

p_T $|\eta|$	5.000 – 10.000	10.000 – 15.000	15.000 – 20.000	20.000 – 25.000	25.000 – 35.000
0.000 – 1.000	0.2760 ± 0.0028	0.2127 ± 0.0024	0.1808 ± 0.0032	0.1541 ± 0.0043	0.1441 ± 0.0009
1.000 – 1.479	0.3119 ± 0.0042	0.2527 ± 0.0036	0.2100 ± 0.0048	0.1820 ± 0.0067	0.1770 ± 0.0015
1.479 – 2.000	0.3340 ± 0.0042	0.2694 ± 0.0037	0.2238 ± 0.0049	0.2197 ± 0.0072	0.2018 ± 0.0016
2.000 – 2.500	0.3343 ± 0.0061	0.2741 ± 0.0054	0.2174 ± 0.0071	0.2012 ± 0.0108	0.2150 ± 0.0027

Table 6: Muon fake rate measured in bins of the muon candidate p_T and η. The uncertainties are statistical only.
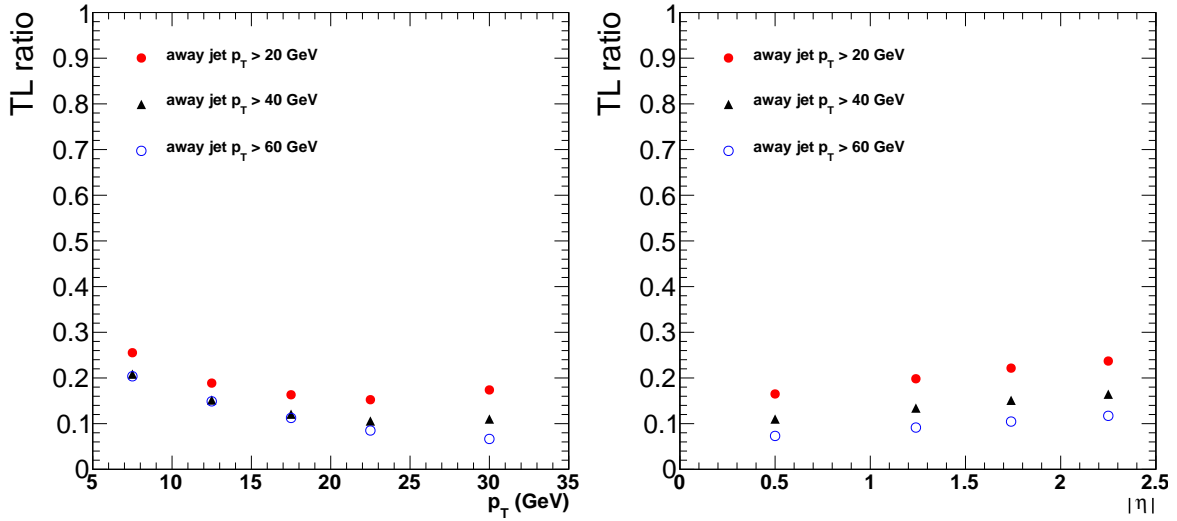
Figure 2: Muon fake rate projected on p_T (left) and $|\eta|$ (right). The fake rates are shown separately for measurements with a requirement for an away jet p_T to be above 20 GeV (red circles), 40 GeV (black circles), and 60 GeV (blue circles).

Figure 3: Electron fake rate projected on p_T (left) and $|\eta|$ (right) for electrons collected by the triggers with calorimeter and tracker isolation requirements (top), with a calorimeter isolation requirement (middle) and without an isolation requirement (bottom). The fake rates are shown separately for measurements with a requirement for an away jet p_T to be above 20 GeV (red filled circles), 40 GeV (black up triangles), and 60 GeV (blue open circles).
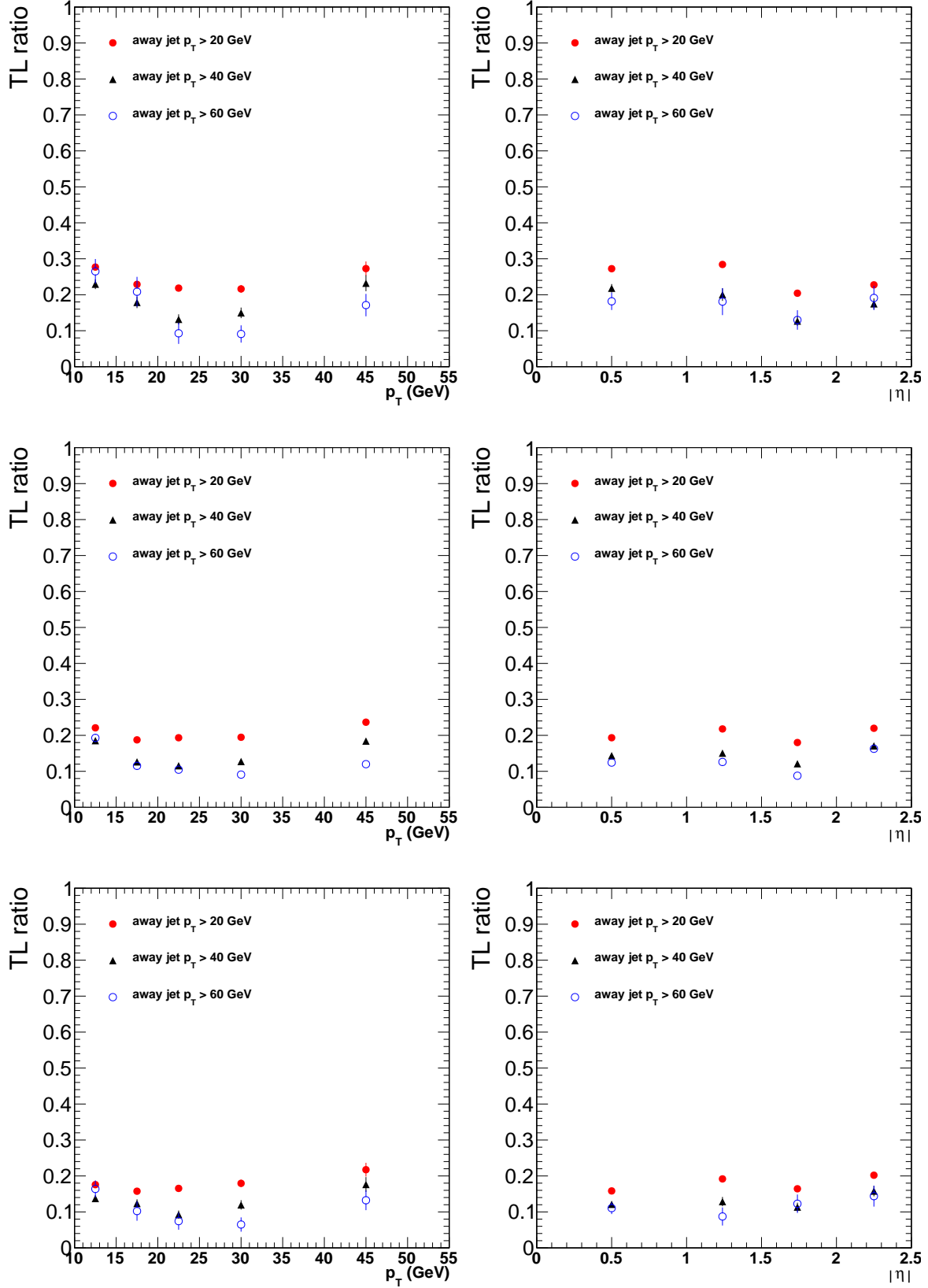
The application of the fake-rate method to predict this background is exactly the same as in the inclusive analysis [3]. As in the inclusive same-sign analysis, the measured fake rates are restricted to $p_T < 55(35)$ GeV for electrons (muons), where we find the contamination from electroweak sources (W/Z production) to be negligible. The values for the highest measured p_T range apply for all leptons with larger momenta. Measurements for lepton $p_T < 20$ GeV are given for completeness, they are not used in the analysis.

THE REST IS NOT UPDATED YET We test that the fake rates measured in QCD are applicable to the dilepton samples by performing closure tests on simulated W+jets, $t\bar{t}$, and QCD samples. The tests done on W+jets and $t\bar{t}$ samples are done as follows

1. select events passing the baseline selections;

2. require that one lepton is matched to a leptonic W decay and the other (fake) lepton is not matched to a leptonic W decay;

3. scale the number of fake leptons failing the full lepton selections and passing the FO selections by $FR/(1 - FR)$ as a function of the fake lepton p_T and $|\eta|$ — this is the prediction of the number of fakes passing full lepton selections;

4. compare the predicted and observed number of fake leptons.

The prediction of the number of events with fakes gives a consistent overestimate for the $t\bar{t}$ events for both electrons and muons by approximately the same fraction of 70% of the observed value, or, equivalently, the observed value differs from the prediction by approximately 40% of the predicted value. We attribute this to the difference in the underlying parton momenta in $t\bar{t}$ and inclusive QCD events: the momentum is generally higher in $t\bar{t}$ events, which corresponds to a smaller effective fake rate. We find that the prediction of the number of fakes gives a marginally significant underestimate for W+jets events. The statistical uncertainty of this test is much larger for muons than for electrons. We expect this to happen if the jets initiating the fakes in W+jet events have a smaller momentum on average compared to those used to extract the fake rate in QCD events. Results of the closure tests on $t\bar{t}$ and W+jet events passing the baseline selections of *high-p_T* dileptons are summarized in Table 7. In addition to this, we have performed a closure test on the same-sign dimuon events in the QCD sample (without any additional requirement on the number of jets or on $\not{E}_T$): we find that the number of expected events agrees with the observed within statistical uncertainty of about 20%.

Sample	result	ElectronFR		Muon FR	
		ee	$e\mu$	$\mu\mu$	$e\mu$
$t\bar{t}$	observed	2.8 ± 0.2	4.2 ± 0.2	3.9 ± 0.2	4.0 ± 0.2
	predicted	4.9 ± 0.4	6.8 ± 0.5	7.2 ± 0.3	6.5 ± 0.2
	ratio	1.8 ± 0.2	1.6 ± 0.2	1.8 ± 0.1	1.6 ± 0.1
W+jets	observed	< 2.1	8.4 ± 4.2	2.1 ± 2.1	
	predicted	1.5 ± 0.8	3.4 ± 1.4	2.1 ± 1.2	
	ratio	< 1.4	0.4 ± 0.3	1.0 ± 1.2	

Table 7: Fake rate closure test on $t\bar{t}$ and W+jets events for high-p_T dilepton selections. The muon FR test in $e\mu$ is done with $\not{E}_T > 20$ GeV. The number of events is scaled to 1 fb^{-1}. Expcept for the test in $t\bar{t}$ with electrons (done with jet $p_T > 40$ GeV), the results are reported for events with at least two jets with $p_T > 30$ GeV (old selection), used to increase the number of events passing the selections.

The systematic uncertainty of $\pm 50\%$ per fake lepton is estimated for the fake rate method. It is justified based on the closure tests and an understanding that the variation of the fake rate on the jet momentum corresponds to the variation between the fakes from the ISR/FSR jets (like in W+jets), and jets from the heavy final states (as in $t\bar{t}$). We compute the contributions from QCD and W+jets and assign a 50% systematic uncertainty on the combined estimate.

We have neglected any "signal contamination". Signal contamination enters when there is a significant source of two isolated leptons, with one or both failing the numerator cuts, but passing the denominator cuts comprising a significant fraction of the total number of $N_{n\bar{n}}$ or $N_{\overline{nn}}$ samples. Without an additional correction that can be easily applied, a contribution from events with two real same-sign dileptons failing the numerator selections will overestimate the background contribution by approximately 3% of the count of the real same-sign dileptons passing the numerator selections. Considering the size of the uncertainty on the background, this effect can be

safely ignored in the estimates of the fake leptons until the rate of same-sign dileptons passing the full selections is at least an order of magnitude higher than that expected from fakes alone.

5.2 Data Driven prediction for charge mis-reconstruction backgrounds

Following our original studies [2] of the electron charge misreconstruction, we apply the requirement for electrons that all three charge measurements for a GSF electron agree. This dramatically reduces the rate of charge mismeasurement for electrons to the point where it is an almost negligible source of background, less than 10% of the background due to fake leptons, as was shown in the 2010 analysis [2]. Even though this background is small, it is not necessarily well-reproduced in simulation. We apply a data-driven method used in the previous analysis here.

The following steps are done:

1. Measure the probability for an electron to have its charge misreconstructed in bins of $|\eta|$ and p_T using single electron gun Monte Carlo.

2. Use this probability and apply it to the opposite sign Z sample for a Z control sample defined as 76 GeV $< m_{ll} < 106$ GeV, $\not{E}_T < 20$ GeV, and transverse mass < 25 GeV. Here transverse mass is calculated based on whichever lepton has higher p_T. Compare with the actual yield of double-charged Z candidates in that region to establish validity of the approach.

3. If the expected and observed yields agree reasonably well in the previous step, continue using the probability measured in the first step and use the discrepancy as a systematic uncertainty.

4. Then apply this probability to all the electrons in opposite sign dilepton events that pass the selection. This produces the data driven charge flip prediction shown in the tables in Section 7.

5. The lepton p_T distributions of leptons from top is slightly harder than that for leptons from Z. The above test thus does not fully sample the lepton spectrum for our background sample. We assign an additional systematics to account for this effect.

Figure 4 shows the p_T (left) and $|\eta|$ (right) projections of the charge mismeasurement probability from single electron gun Monte Carlo. The same function is applied to data and MC. As seen in Fig. 4 (right), the charge mismeasurement probability did not change substantially in the samples used for the previous analysis, as well as for the Spring11 and Summer11 simulation.
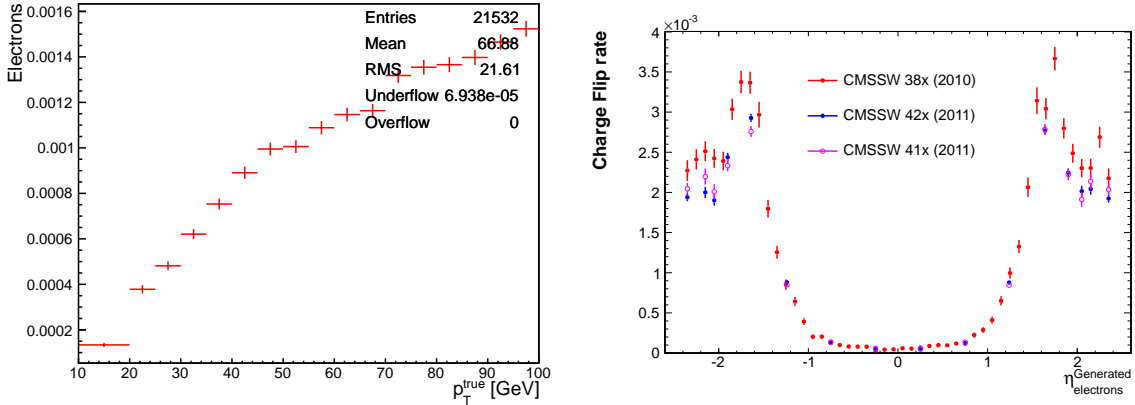
Figure 4: Charge mismeasurement probability from single electron gun MC shown in projections on p_T (left) and η (right). The projection on η also shows the distributions for the charge mismeasurement probability in 2010 analysis (red), current definition (blue), and that in the older (Spring11-like) MC sample.

We find 390 events with same-sign electron pairs in data in the Z control region. This needs to be compared with the sum of the expected same-sign events as estimated from opposite-sign dielectrons, 359.7 ± 4.1, plus a contribution from fakes, 11 ± 6. The number of events expected directly from simulation is 469 ± 11. The same-sign dielectron mass distribution observed in data is compared to the expectation from simulation in Fig. 5. These comparisons are consistent within statistics. The uncertainty is taken to be 20% to account for kinematic differences between leptons from Drell-Yan events and top pairs, the latter expected to be the dominant source of background events for this analysis.

10
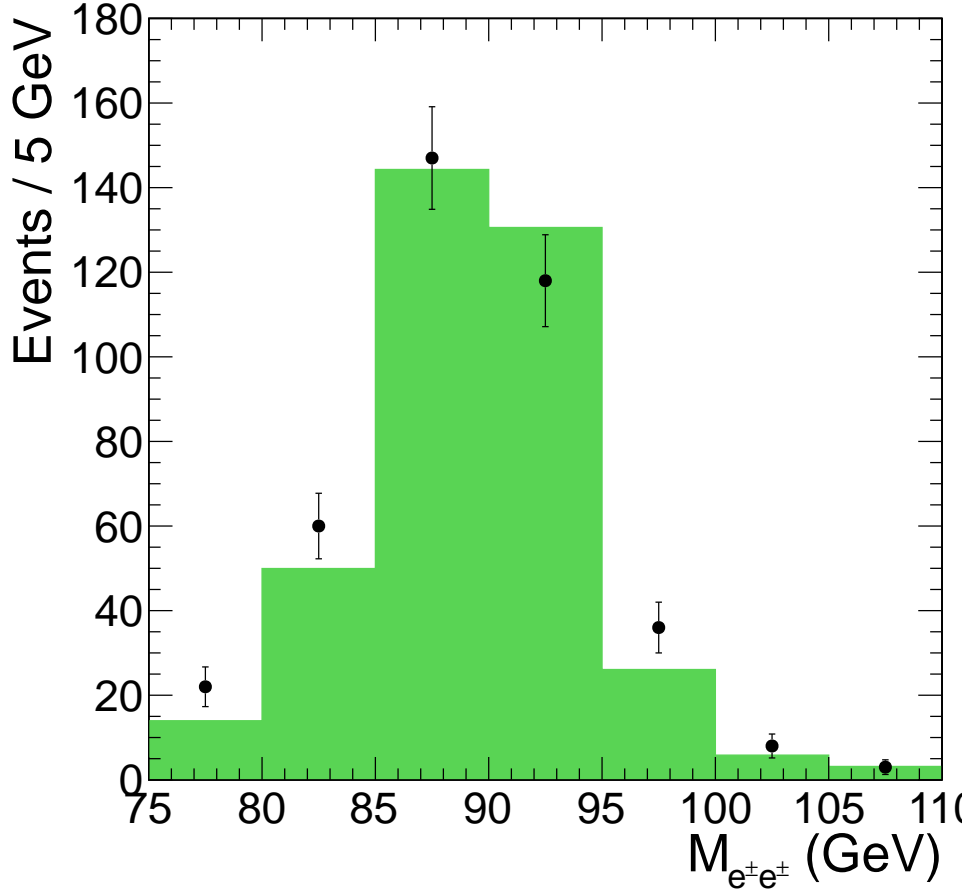
Figure 5: Same sign ee invariant mass distribution compared with $Z \rightarrow ee$ Monte Carlo expectations. Cuts on missing transverse energy < 20 GeV and transverse mass < 25 GeV have been applied to reduce backgrounds from $W+$ jets. The highest p_T lepton has been used in the calculation of the transverse mass.

6 Acceptance Systematics

Systematic uncertainties arise from uncertainties on event selections expected in simulation compared to the actual performance of the detector. As this search is in many ways similar to the inclusive same-sign dilepton search [3], our treatment of efficiency systematics parallels the one in that analysis. In this section, we briefly summarize those results, and describe the uncertainties due to the b-tagging requirement.

For the inclusive search without a well-defined signal, we evaluate the systematics with reference to the SUSY benchmark point LM9, as well as opposite sign $t\bar{t}$ simulation, both of which have b-enriched event topologies. The CMS benchmark point LM9 defines the common scalar mass (m0) = 1.45 TeV, the common gaugino mass (m1/2) = 175 GeV, the ratio of the Higgs expectation values ($\tan\beta$) = 10, tri-linear coupling (A0) = 0 and the sign of the Higgsino mass parameter (μ) > 0. This produces heavy squarks with light gluinos leading to several heavy flavor final states.

For the b-tagging efficiency as well as the systematic uncertainties we refer to the work by the BTV POG group for 2011 data [5]. In that study they provide the uncertainties on b-tagging efficiency, as well as scale factors (SF) for $t\bar{t}$ events. In Fig. 6 we compare the leading jet p_T normalized distribution for LM9 using the same-sign dilepton selection. For the $t\bar{t}$ events, we explicitely use opposite-sign dileptons in order to gain statistics. Given that the bulk of the p_T range accessible by LM9 is also covered by the $t\bar{t}$ decays, we consider 8.0% as the systematic uncertainty on the efficiency (per b-jet) from PtRel measurements [5]. We thus use the measurement of scale factors (SFs) for $t\bar{t}$ for the inclusive search.

Once we have all the various signal MCs we mention in Section 9, we will replace Figure 6 with one that compares all of these models, and revisit the statement about b-tagging systematics. It is likely that we will adopt different systematics for different models, given the differences in jet p_T for the different models.

11
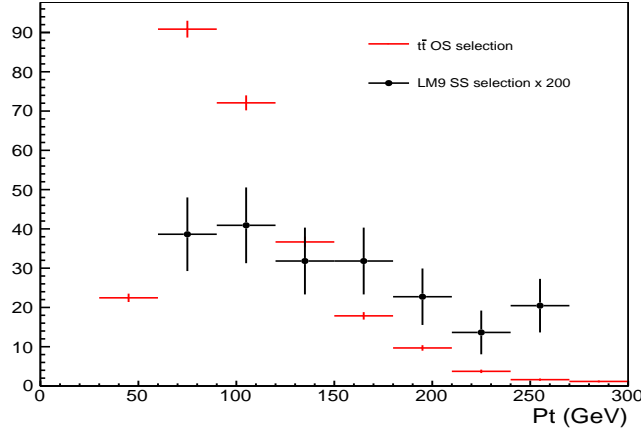
Figure 6: Differential distributions of leading b-tag jet p_T for the LM9 benchmark point and $t\bar{t}$ simulations using 349 pb^{-1} of luminosity normalization.

A complete summary of systematic uncertainties is given in Table 8.

Table 8: Summary of systematic uncertainties on the signal selection and expectation. Reported values are fractional, relative to the total cross section. The values in parentheses are for electrons with p_T below 20 GeV and muons with p_T below 15 GeV for muons.

Source	ee	$\mu\mu$	$e\mu$	all
Lepton selection	11(15)%	11(15)%	11(15)%	11(15)%
Energy scale	5%	5%	5%	5%
ISR/FSR and PDF	2%	2%	2%	2%
b-tag selection	16%	16%	16%	16%
Total without luminosity	20(23)%	20(23)%	20(23)	20(23)%
Integrated luminosity	6%	6%	6%	6%
Total	21(24)%	21(24)%	21(24)%	21(24)%

7 Event Yields and Background Estimation

The results of this search in the above-mentioned kinematical region are summerized in Table **??**. As mentioned in the introduction, and quantified by this table, SM background is expected to be dominated by $t\bar{t}$ production with one real and one fake lepton. We estimate this background from the data itself using the "Tight-To-Loose ratio" (Fake Rate) method [6]. Electron charge mis-reconstruction is estimated by weighting opposite-sign dilepton events that pass all our cuts by a charge flip rate obtained form single electron Monte Carlo as described in detail in [3]. The probability for muons to be reconstructed with the wrong sign in the relevant momemtum range is negligible. Both of these techniques are described in more detail in [3]. Systematic errors on these two estimates are 50% and 25% respectively.

Source	ee	$\mu\mu$	eμ	all
$t\bar{t} \to \ell\ell X$	0.469 ± 0.305	0.000 ± 0.199	1.133 ± 0.580	1.603 ± 0.656
$t\bar{t}$ other	0.000 ± 0.199	0.000 ± 0.199	0.000 ± 0.199	0.000 ± 0.199
$t\bar{t} \to \ell(b \to \ell)X$	0.000 ± 0.199	0.193 ± 0.143	0.000 ± 0.199	0.193 ± 0.143
$t\bar{t} \to \ell(\not{b} \to \ell)X$	0.563 ± 0.399	0.000 ± 0.199	0.143 ± 0.131	0.706 ± 0.420
t, s-channel	0.000 ± 0.057	0.000 ± 0.057	0.000 ± 0.057	0.000 ± 0.057
t, t-channel	0.077 ± 0.077	0.000 ± 0.055	0.000 ± 0.055	0.077 ± 0.077
tW	0.000 ± 0.045	0.000 ± 0.045	0.016 ± 0.045	0.016 ± 0.045
$Z \to ee$	0.000 ± 0.429	0.000 ± 0.429	0.000 ± 0.429	0.000 ± 0.429
$Z \to \mu\mu$	0.000 ± 0.429	0.000 ± 0.429	0.000 ± 0.429	0.000 ± 0.429
$Z \to \tau\tau$	0.000 ± 0.429	0.000 ± 0.429	0.000 ± 0.429	0.000 ± 0.429
W+jets	0.000 ± 1.808	0.000 ± 1.808	0.000 ± 1.808	0.000 ± 1.808
WW	0.000 ± 0.019	0.000 ± 0.019	0.000 ± 0.019	0.000 ± 0.019
$V\gamma$	0.000 ± 0.248	0.000 ± 0.248	0.000 ± 0.248	0.000 ± 0.248
$W\gamma^* \to \ell\nu ee$	0.000 ± 0.097	0.000 ± 0.097	0.000 ± 0.097	0.000 ± 0.097
$W\gamma^* \to \ell\nu\mu\mu$	0.000 ± 0.075	0.000 ± 0.075	0.000 ± 0.075	0.000 ± 0.075
$W\gamma^* \to \ell\nu\tau\tau$	0.000 ± 0.028	0.000 ± 0.028	0.000 ± 0.028	0.000 ± 0.028
WZ	0.034 ± 0.012	0.017 ± 0.008	0.031 ± 0.012	0.082 ± 0.019
ZZ	0.000 ± 0.000	0.001 ± 0.001	0.002 ± 0.001	0.003 ± 0.001
$dpW^{\pm}W^{\pm}$	0.000 ± 0.004	0.000 ± 0.004	0.000 ± 0.004	0.000 ± 0.004
spW^-W^-	0.000 ± 0.001	0.000 ± 0.001	0.003 ± 0.002	0.003 ± 0.002
spW^+W^+	0.000 ± 0.006	0.000 ± 0.006	0.000 ± 0.006	0.000 ± 0.006
$t\bar{t}\gamma$	0.000 ± 0.059	0.000 ± 0.059	0.000 ± 0.059	0.000 ± 0.059
$t\bar{t}W$	0.572 ± 0.025	0.733 ± 0.028	1.286 ± 0.038	2.591 ± 0.053
$t\bar{t}Z$	0.118 ± 0.009	0.158 ± 0.010	0.268 ± 0.013	0.544 ± 0.019
$WW\gamma$	0.000 ± 0.015	0.000 ± 0.015	0.000 ± 0.015	0.000 ± 0.015
WWW	0.001 ± 0.000	0.001 ± 0.000	0.001 ± 0.001	0.003 ± 0.001
WWZ	0.000 ± 0.000	0.000 ± 0.000	0.001 ± 0.001	0.001 ± 0.001
WZZ	0.000 ± 0.000	0.001 ± 0.000	0.001 ± 0.000	0.002 ± 0.001
ZZZ	0.000 ± 0.000	0.000 ± 0.000	0.000 ± 0.000	0.000 ± 0.000
Total MC	1.834 ± 0.509	1.103 ± 0.146	2.885 ± 0.597	5.822 ± 0.797
LM6	0.000 ± 0.000	0.186 ± 0.186	0.383 ± 0.275	0.569 ± 0.332
SF	1.13 ± 0.67	0.30 ± 0.20	1.92 ± 0.74	3.36 ± 1.02
DF	0.04 ± 0.12	0.02 ± 0.02	0.02 ± 0.09	0.08 ± 0.16
SF + DF	$1.17 \pm 0.63 \pm 0.58$	$0.32 \pm 0.20 \pm 0.16$	$1.95 \pm 0.72 \pm 0.97$	$3.43 \pm 0.98 \pm 1.72$
Charge Flips	$0.390 \pm 0.032 \pm 0.078$	$- \pm -$	$0.544 \pm 0.032 \pm 0.109$	$0.934 \pm 0.045 \pm 0.187$
MC Pred	$0.725 \pm 0.029 \pm 0.362$	$0.912 \pm 0.031 \pm 0.456$	$1.595 \pm 0.042 \pm 0.797$	$3.231 \pm 0.059 \pm 1.616$
Total Pred	$2.281 \pm 0.633 \pm 0.691$	$1.232 \pm 0.199 \pm 0.483$	$4.086 \pm 0.725 \pm 1.263$	$7.600 \pm 0.983 \pm 2.365$
data	2	2	3	7

Table 9: Observed event yields in baseline ($\not{E}_T > 30$ GeV, at least 2 jets with pT > 40 GeV, and at least two of these jets b-tagged using SSVHEM) high-p_T (pT $> 20/20$) dileptons compared to expectations from simulation alone, and from the data-driven methods. The *simulated backgrounds* contribution includes contributions from genuine same-sign lepton pairs (WZ, ZZ, leptons from same-sign W from single-parton, double-parton, and $t\bar{t}W$ production, etc.), as well as electrons from converted photons in $V\gamma$ production. Entries with zero contributing events are reported with an uncertainty corresponding to one event. This uncertainty is not added to the total MC contribution. Systematic uncertainties (the second uncertainty if present) are displayed only for the final combined type of background, no systematic uncertainty is added for estimates with zero entries. Systematic uncertainties are 100% correlated among the channels.

Source	ee	$\mu\mu$	eμ	all
$t\bar{t} \to \ell\ell X$	0.071 ± 0.199	0.000 ± 0.199	0.000 ± 0.199	0.071 ± 0.199
$t\bar{t}$ other	0.000 ± 0.199	0.000 ± 0.199	0.000 ± 0.199	0.000 ± 0.199
$t\bar{t} \to \ell(b \to \ell)X$	0.000 ± 0.199	0.000 ± 0.199	0.000 ± 0.199	0.000 ± 0.199
$t\bar{t} \to \ell(\bar{b} \to \ell)X$	0.272 ± 0.272	0.000 ± 0.199	0.130 ± 0.130	0.402 ± 0.301
t, s-channel	0.000 ± 0.057	0.000 ± 0.057	0.000 ± 0.057	0.000 ± 0.057
t, t-channel	0.000 ± 0.055	0.000 ± 0.055	0.000 ± 0.055	0.000 ± 0.055
tW	0.000 ± 0.045	0.000 ± 0.045	0.000 ± 0.045	0.000 ± 0.045
$Z \to ee$	0.000 ± 0.429	0.000 ± 0.429	0.000 ± 0.429	0.000 ± 0.429
$Z \to \mu\mu$	0.000 ± 0.429	0.000 ± 0.429	0.000 ± 0.429	0.000 ± 0.429
$Z \to \tau\tau$	0.000 ± 0.429	0.000 ± 0.429	0.000 ± 0.429	0.000 ± 0.429
W+jets	0.000 ± 1.808	0.000 ± 1.808	0.000 ± 1.808	0.000 ± 1.808
WW	0.000 ± 0.019	0.000 ± 0.019	0.000 ± 0.019	0.000 ± 0.019
$V\gamma$	0.000 ± 0.248	0.000 ± 0.248	0.000 ± 0.248	0.000 ± 0.248
$W\gamma^* \to \ell\nu ee$	0.000 ± 0.097	0.000 ± 0.097	0.000 ± 0.097	0.000 ± 0.097
$W\gamma^* \to \ell\nu\mu\mu$	0.000 ± 0.075	0.000 ± 0.075	0.000 ± 0.075	0.000 ± 0.075
$W\gamma^* \to \ell\nu\tau\tau$	0.000 ± 0.028	0.000 ± 0.028	0.000 ± 0.028	0.000 ± 0.028
WZ	0.009 ± 0.006	0.001 ± 0.003	0.006 ± 0.004	0.016 ± 0.008
ZZ	0.000 ± 0.000	0.000 ± 0.000	0.000 ± 0.000	0.000 ± 0.000
dp$W^{\pm}W^{\pm}$	0.000 ± 0.004	0.000 ± 0.004	0.000 ± 0.004	0.000 ± 0.004
spW^-W^-	0.000 ± 0.001	0.000 ± 0.001	0.001 ± 0.001	0.001 ± 0.001
spW^+W^+	0.000 ± 0.006	0.000 ± 0.006	0.000 ± 0.006	0.000 ± 0.006
$t\bar{t}\gamma$	0.000 ± 0.059	0.000 ± 0.059	0.000 ± 0.059	0.000 ± 0.059
$t\bar{t}W$	0.200 ± 0.015	0.214 ± 0.015	0.416 ± 0.021	0.831 ± 0.030
$t\bar{t}Z$	0.037 ± 0.005	0.055 ± 0.006	0.094 ± 0.008	0.186 ± 0.011
$WW\gamma$	0.000 ± 0.015	0.000 ± 0.015	0.000 ± 0.015	0.000 ± 0.015
WWW	0.000 ± 0.000	0.000 ± 0.000	0.001 ± 0.001	0.002 ± 0.001
WWZ	0.000 ± 0.000	0.000 ± 0.000	0.000 ± 0.000	0.000 ± 0.000
WZZ	0.000 ± 0.000	0.000 ± 0.000	0.000 ± 0.000	0.000 ± 0.000
ZZZ	0.000 ± 0.000	0.000 ± 0.000	0.000 ± 0.000	0.000 ± 0.000
Total MC	0.589 ± 0.281	0.271 ± 0.016	0.649 ± 0.132	1.509 ± 0.311
LM6	0.000 ± 0.000	0.186 ± 0.186	0.383 ± 0.275	0.569 ± 0.332
SF	0.27 ± 0.54	0.00 ± 0.37	0.54 ± 0.59	0.81 ± 0.74
DF	0.00 ± 0.14	0.00 ± 0.10	0.00 ± 0.16	0.00 ± 0.16
SF + DF	$0.27 \pm 0.45 \pm 0.14$	$0.00 \pm 0.31 \pm 0.00$	$0.54 \pm 0.50 \pm 0.27$	$0.81 \pm 0.67 \pm 0.40$
Charge Flips	$0.036 \pm 0.010 \pm 0.007$	$- \pm -$	$0.069 \pm 0.012 \pm 0.014$	$0.104 \pm 0.015 \pm 0.021$
MC Pred	$0.247 \pm 0.017 \pm 0.123$	$0.271 \pm 0.016 \pm 0.135$	$0.519 \pm 0.023 \pm 0.260$	$1.037 \pm 0.033 \pm 0.518$
Total Pred	$0.555 \pm 0.453 \pm 0.184$	$0.271 \pm 0.315 \pm 0.135$	$1.123 \pm 0.496 \pm 0.373$	$1.949 \pm 0.672 \pm 0.658$
data	1	1	0	2

Table 10: Observed event yields in high-p_T (pT > 20/20) dileptons passing the *low-m_0* signal selections ($H_T > 320$ GeV, $\not{E}_T > 50$ GeV) compared to expectations from simulation alone, and from the data-driven methods. The *simulated backgrounds* contribution includes contributions from genuine same-sign lepton pairs (WZ, ZZ, leptons from same-sign W from single-, double-parton, and $t\bar{t}W$ production, etc.), as well as electrons from converted photons in $V\gamma$ production. Entries with zero contributing events are reported with an uncertainty corresponding to one event. This uncertainty is not added to the total MC contribution. Systematic uncertainties (the second uncertainty if present) are displayed only for the final combined type of background, no systematic uncertainty is added for estimates with zero entries. Systematic uncertainties are 100% correlated among the channels.

14

Source	ee	$\mu\mu$	eμ	all
$t\bar{t} \to \ell\ell X$	0.000 ± 0.199	0.000 ± 0.199	0.000 ± 0.199	0.000 ± 0.199
$t\bar{t}$ other	0.000 ± 0.199	0.000 ± 0.199	0.000 ± 0.199	0.000 ± 0.199
$t\bar{t} \to \ell(b \to \ell)X$	0.000 ± 0.199	0.000 ± 0.199	0.000 ± 0.199	0.000 ± 0.199
$t\bar{t} \to \ell(\bar{b} \to \ell)X$	0.272 ± 0.272	0.000 ± 0.199	0.000 ± 0.199	0.272 ± 0.272
t, s-channel	0.000 ± 0.057	0.000 ± 0.057	0.000 ± 0.057	0.000 ± 0.057
t, t-channel	0.000 ± 0.055	0.000 ± 0.055	0.000 ± 0.055	0.000 ± 0.055
tW	0.000 ± 0.045	0.000 ± 0.045	0.000 ± 0.045	0.000 ± 0.045
$Z \to ee$	0.000 ± 0.429	0.000 ± 0.429	0.000 ± 0.429	0.000 ± 0.429
$Z \to \mu\mu$	0.000 ± 0.429	0.000 ± 0.429	0.000 ± 0.429	0.000 ± 0.429
$Z \to \tau\tau$	0.000 ± 0.429	0.000 ± 0.429	0.000 ± 0.429	0.000 ± 0.429
W+jets	0.000 ± 1.808	0.000 ± 1.808	0.000 ± 1.808	0.000 ± 1.808
WW	0.000 ± 0.019	0.000 ± 0.019	0.000 ± 0.019	0.000 ± 0.019
Vγ	0.000 ± 0.248	0.000 ± 0.248	0.000 ± 0.248	0.000 ± 0.248
$W\gamma^* \to \ell\nu ee$	0.000 ± 0.097	0.000 ± 0.097	0.000 ± 0.097	0.000 ± 0.097
$W\gamma^* \to \ell\nu\mu\mu$	0.000 ± 0.075	0.000 ± 0.075	0.000 ± 0.075	0.000 ± 0.075
$W\gamma^* \to \ell\nu\tau\tau$	0.000 ± 0.028	0.000 ± 0.028	0.000 ± 0.028	0.000 ± 0.028
WZ	0.000 ± 0.003	0.001 ± 0.003	0.004 ± 0.004	0.005 ± 0.004
ZZ	0.000 ± 0.000	0.000 ± 0.000	0.000 ± 0.000	0.000 ± 0.000
dp$W^{\pm}W^{\pm}$	0.000 ± 0.004	0.000 ± 0.004	0.000 ± 0.004	0.000 ± 0.004
spW^-W^-	0.000 ± 0.001	0.000 ± 0.001	0.001 ± 0.001	0.001 ± 0.001
spW^+W^+	0.000 ± 0.006	0.000 ± 0.006	0.000 ± 0.006	0.000 ± 0.006
$t\bar{t}\gamma$	0.000 ± 0.059	0.000 ± 0.059	0.000 ± 0.059	0.000 ± 0.059
$t\bar{t}W$	0.099 ± 0.011	0.097 ± 0.010	0.184 ± 0.014	0.379 ± 0.020
$t\bar{t}Z$	0.020 ± 0.004	0.028 ± 0.004	0.049 ± 0.005	0.098 ± 0.008
$WW\gamma$	0.000 ± 0.015	0.000 ± 0.015	0.000 ± 0.015	0.000 ± 0.015
WWW	0.000 ± 0.000	0.000 ± 0.000	0.000 ± 0.000	0.001 ± 0.001
WWZ	0.000 ± 0.000	0.000 ± 0.000	0.000 ± 0.000	0.000 ± 0.000
WZZ	0.000 ± 0.000	0.000 ± 0.000	0.000 ± 0.000	0.000 ± 0.000
ZZZ	0.000 ± 0.000	0.000 ± 0.000	0.000 ± 0.000	0.000 ± 0.000
Total MC	0.391 ± 0.272	0.126 ± 0.011	0.239 ± 0.015	0.756 ± 0.273
LM6	0.000 ± 0.000	0.186 ± 0.186	0.383 ± 0.275	0.569 ± 0.332
SF	0.00 ± 0.58	0.00 ± 0.37	0.15 ± 0.54	0.15 ± 0.54
DF	0.00 ± 0.14	0.00 ± 0.10	0.00 ± 0.16	0.00 ± 0.16
SF + DF	$0.00 \pm 0.50 \pm 0.00$	$0.00 \pm 0.31 \pm 0.00$	$0.15 \pm 0.44 \pm 0.07$	$0.15 \pm 0.44 \pm 0.07$
Charge Flips	$0.011 \pm 0.004 \pm 0.002$	$- \pm -$	$0.016 \pm 0.005 \pm 0.003$	$0.027 \pm 0.006 \pm 0.005$
MC Pred	$0.119 \pm 0.011 \pm 0.060$	$0.126 \pm 0.011 \pm 0.063$	$0.239 \pm 0.015 \pm 0.119$	$0.485 \pm 0.022 \pm 0.242$
Total Pred	$0.130 \pm 0.501 \pm 0.060$	$0.126 \pm 0.315 \pm 0.063$	$0.404 \pm 0.438 \pm 0.141$	$0.661 \pm 0.438 \pm 0.254$
data	1	0	0	1

Table 11: Observed event yields in high-p_T (pT > 20/20) dileptons passing the *high-m_0* signal selections ($H_T >$ 440 GeV, $\not{E}_T >$ 50 GeV) compared to expectations from simulation alone, and from the data-driven methods. The *simulated backgrounds* contribution includes contributions from genuine same-sign lepton pairs (WZ, ZZ, leptons from same-sign W from single-, double-parton, and $t\bar{t}W$ production, etc.), as well as electrons from converted photons in $V\gamma$ production. Entries with zero contributing events are reported with an uncertainty corresponding to one event. This uncertainty is not added to the total MC contribution. Systematic uncertainties (the second uncertainty if present) are displayed only for the final combined type of background, no systematic uncertainty is added for estimates with zero entries. Systematic uncertainties are 100% correlated among the channels.

15

Source	ee	$\mu\mu$	eμ	all
$t\bar{t} \to \ell\ell X$	0.000 ± 0.199	0.000 ± 0.199	0.000 ± 0.199	0.000 ± 0.199
$t\bar{t}$ other	0.000 ± 0.199	0.000 ± 0.199	0.000 ± 0.199	0.000 ± 0.199
$t\bar{t} \to \ell(b \to \ell)X$	0.000 ± 0.199	0.000 ± 0.199	0.000 ± 0.199	0.000 ± 0.199
$t\bar{t} \to \ell(\bar{b} \to \ell)X$	0.000 ± 0.199	0.000 ± 0.199	0.000 ± 0.199	0.000 ± 0.199
t, s-channel	0.000 ± 0.057	0.000 ± 0.057	0.000 ± 0.057	0.000 ± 0.057
t, t-channel	0.000 ± 0.055	0.000 ± 0.055	0.000 ± 0.055	0.000 ± 0.055
tW	0.000 ± 0.045	0.000 ± 0.045	0.000 ± 0.045	0.000 ± 0.045
$Z \to ee$	0.000 ± 0.429	0.000 ± 0.429	0.000 ± 0.429	0.000 ± 0.429
$Z \to \mu\mu$	0.000 ± 0.429	0.000 ± 0.429	0.000 ± 0.429	0.000 ± 0.429
$Z \to \tau\tau$	0.000 ± 0.429	0.000 ± 0.429	0.000 ± 0.429	0.000 ± 0.429
W+jets	0.000 ± 1.808	0.000 ± 1.808	0.000 ± 1.808	0.000 ± 1.808
WW	0.000 ± 0.019	0.000 ± 0.019	0.000 ± 0.019	0.000 ± 0.019
$V\gamma$	0.000 ± 0.248	0.000 ± 0.248	0.000 ± 0.248	0.000 ± 0.248
$W\gamma^* \to \ell\nu ee$	0.000 ± 0.097	0.000 ± 0.097	0.000 ± 0.097	0.000 ± 0.097
$W\gamma^* \to \ell\nu\mu\mu$	0.000 ± 0.075	0.000 ± 0.075	0.000 ± 0.075	0.000 ± 0.075
$W\gamma^* \to \ell\nu\tau\tau$	0.000 ± 0.028	0.000 ± 0.028	0.000 ± 0.028	0.000 ± 0.028
WZ	0.010 ± 0.007	0.001 ± 0.003	0.000 ± 0.003	0.011 ± 0.007
ZZ	0.000 ± 0.000	0.000 ± 0.000	0.001 ± 0.001	0.001 ± 0.001
$dpW^{\pm}W^{\pm}$	0.000 ± 0.004	0.000 ± 0.004	0.000 ± 0.004	0.000 ± 0.004
spW^-W^-	0.000 ± 0.001	0.000 ± 0.001	0.001 ± 0.001	0.001 ± 0.001
spW^+W^+	0.000 ± 0.006	0.000 ± 0.006	0.000 ± 0.006	0.000 ± 0.006
$t\bar{t}\gamma$	0.000 ± 0.059	0.000 ± 0.059	0.000 ± 0.059	0.000 ± 0.059
$t\bar{t}W$	0.097 ± 0.010	0.121 ± 0.011	0.244 ± 0.016	0.462 ± 0.022
$t\bar{t}Z$	0.016 ± 0.003	0.023 ± 0.004	0.041 ± 0.005	0.079 ± 0.007
$WW\gamma$	0.000 ± 0.015	0.000 ± 0.015	0.000 ± 0.015	0.000 ± 0.015
WWW	0.000 ± 0.000	0.000 ± 0.000	0.000 ± 0.000	0.001 ± 0.000
WWZ	0.000 ± 0.000	0.000 ± 0.000	0.000 ± 0.000	0.000 ± 0.000
WZZ	0.000 ± 0.000	0.000 ± 0.000	0.000 ± 0.000	0.000 ± 0.000
ZZZ	0.000 ± 0.000	0.000 ± 0.000	0.000 ± 0.000	0.000 ± 0.000
Total MC	0.123 ± 0.013	0.145 ± 0.012	0.288 ± 0.017	0.555 ± 0.024
LM6	0.000 ± 0.000	0.186 ± 0.186	0.383 ± 0.275	0.569 ± 0.332
SF	0.00 ± 0.58	0.00 ± 0.37	0.32 ± 0.57	0.32 ± 0.57
DF	0.00 ± 0.14	0.00 ± 0.10	0.00 ± 0.16	0.00 ± 0.16
SF + DF	$0.00 \pm 0.50 \pm 0.00$	$0.00 \pm 0.31 \pm 0.00$	$0.32 \pm 0.47 \pm 0.16$	$0.32 \pm 0.47 \pm 0.16$
Charge Flips	$0.021 \pm 0.007 \pm 0.004$	$- \pm -$	$0.022 \pm 0.006 \pm 0.004$	$0.043 \pm 0.009 \pm 0.009$
MC Pred	$0.123 \pm 0.013 \pm 0.061$	$0.145 \pm 0.012 \pm 0.072$	$0.288 \pm 0.017 \pm 0.144$	$0.555 \pm 0.024 \pm 0.278$
Total Pred	$0.144 \pm 0.501 \pm 0.061$	$0.145 \pm 0.315 \pm 0.072$	$0.634 \pm 0.474 \pm 0.217$	$0.923 \pm 0.474 \pm 0.322$
data	1	0	1	2

Table 12: Observed event yields in high-p_T (pT > 20/20) dileptons passing the *simplified model* signal selections ($H_T > 200$ GeV, $\not{E}_T > 120$ GeV) compared to expectations from simulation alone, and from the data-driven methods. The *simulated backgrounds* contribution includes contributions from genuine same-sign lepton pairs (WZ, ZZ, leptons from same-sign W from single-, double-parton, and $t\bar{t}W$ production, etc.), as well as electrons from converted photons in $V\gamma$ production. Entries with zero contributing events are reported with an uncertainty corresponding to one event. This uncertainty is not added to the total MC contribution. Systematic uncertainties (the second uncertainty if present) are displayed only for the final combined type of background, no systematic uncertainty is added for estimates with zero entries. Systematic uncertainties are 100% correlated among the channels.

Source	ee	$\mu\mu$	eμ	all
$t\bar{t} \to \ell\ell X$	0.000 ± 0.199	0.000 ± 0.199	0.000 ± 0.199	0.000 ± 0.199
$t\bar{t}$ other	0.000 ± 0.199	0.000 ± 0.199	0.000 ± 0.199	0.000 ± 0.199
$t\bar{t} \to \ell(b \to \ell)X$	0.000 ± 0.199	0.000 ± 0.199	0.000 ± 0.199	0.000 ± 0.199
$t\bar{t} \to \ell(\bar{b} \to \ell)X$	0.000 ± 0.199	0.000 ± 0.199	0.000 ± 0.199	0.000 ± 0.199
t, s-channel	0.000 ± 0.057	0.000 ± 0.057	0.000 ± 0.057	0.000 ± 0.057
t, t-channel	0.000 ± 0.055	0.000 ± 0.055	0.000 ± 0.055	0.000 ± 0.055
tW	0.000 ± 0.045	0.000 ± 0.045	0.000 ± 0.045	0.000 ± 0.045
$Z \to ee$	0.000 ± 0.429	0.000 ± 0.429	0.000 ± 0.429	0.000 ± 0.429
$Z \to \mu\mu$	0.000 ± 0.429	0.000 ± 0.429	0.000 ± 0.429	0.000 ± 0.429
$Z \to \tau\tau$	0.000 ± 0.429	0.000 ± 0.429	0.000 ± 0.429	0.000 ± 0.429
W+jets	0.000 ± 1.808	0.000 ± 1.808	0.000 ± 1.808	0.000 ± 1.808
WW	0.000 ± 0.019	0.000 ± 0.019	0.000 ± 0.019	0.000 ± 0.019
$V\gamma$	0.000 ± 0.248	0.000 ± 0.248	0.000 ± 0.248	0.000 ± 0.248
$W\gamma^* \to \ell\nu ee$	0.000 ± 0.097	0.000 ± 0.097	0.000 ± 0.097	0.000 ± 0.097
$W\gamma^* \to \ell\nu\mu\mu$	0.000 ± 0.075	0.000 ± 0.075	0.000 ± 0.075	0.000 ± 0.075
$W\gamma^* \to \ell\nu\tau\tau$	0.000 ± 0.028	0.000 ± 0.028	0.000 ± 0.028	0.000 ± 0.028
WZ	0.004 ± 0.004	0.001 ± 0.003	0.000 ± 0.003	0.006 ± 0.005
ZZ	0.000 ± 0.000	0.000 ± 0.000	0.000 ± 0.000	0.000 ± 0.000
$dpW^{\pm}W^{\pm}$	0.000 ± 0.004	0.000 ± 0.004	0.000 ± 0.004	0.000 ± 0.004
spW^-W^-	0.000 ± 0.001	0.000 ± 0.001	0.001 ± 0.001	0.001 ± 0.001
spW^+W^+	0.000 ± 0.006	0.000 ± 0.006	0.000 ± 0.006	0.000 ± 0.006
$t\bar{t}\gamma$	0.000 ± 0.059	0.000 ± 0.059	0.000 ± 0.059	0.000 ± 0.059
$t\bar{t}W$	0.069 ± 0.009	0.080 ± 0.009	0.168 ± 0.013	0.317 ± 0.018
$t\bar{t}Z$	0.013 ± 0.003	0.014 ± 0.003	0.033 ± 0.005	0.060 ± 0.006
$WW\gamma$	0.000 ± 0.015	0.000 ± 0.015	0.000 ± 0.015	0.000 ± 0.015
WWW	0.000 ± 0.000	0.000 ± 0.000	0.000 ± 0.000	0.001 ± 0.000
WWZ	0.000 ± 0.000	0.000 ± 0.000	0.000 ± 0.000	0.000 ± 0.000
WZZ	0.000 ± 0.000	0.000 ± 0.000	0.000 ± 0.000	0.000 ± 0.000
ZZZ	0.000 ± 0.000	0.000 ± 0.000	0.000 ± 0.000	0.000 ± 0.000
Total MC	0.086 ± 0.010	0.096 ± 0.010	0.203 ± 0.014	0.385 ± 0.020
LM6	0.000 ± 0.000	0.186 ± 0.186	0.383 ± 0.275	0.569 ± 0.332
SF	0.00 ± 0.58	0.00 ± 0.37	0.15 ± 0.54	0.15 ± 0.54
DF	0.00 ± 0.14	0.00 ± 0.10	0.00 ± 0.16	0.00 ± 0.16
SF + DF	$0.00 \pm 0.50 \pm 0.00$	$0.00 \pm 0.31 \pm 0.00$	$0.15 \pm 0.44 \pm 0.07$	$0.15 \pm 0.44 \pm 0.07$
Charge Flips	$0.014 \pm 0.006 \pm 0.003$	$- \pm -$	$0.011 \pm 0.005 \pm 0.002$	$0.025 \pm 0.008 \pm 0.005$
MC Pred	$0.087 \pm 0.010 \pm 0.043$	$0.096 \pm 0.010 \pm 0.048$	$0.203 \pm 0.014 \pm 0.101$	$0.385 \pm 0.020 \pm 0.192$
Total Pred	$0.101 \pm 0.501 \pm 0.043$	$0.096 \pm 0.315 \pm 0.048$	$0.364 \pm 0.438 \pm 0.126$	$0.560 \pm 0.438 \pm 0.206$
data	0	0	0	0

Table 13: Observed event yields in high-p_T (pT > 20/20) dileptons passing the *pMSSW/sneutrino* signal selections ($H_T > 320$ GeV, $\not{E}_T > 120$ GeV) compared to expectations from simulation alone, and from the data-driven methods. The *simulated backgrounds* contribution includes contributions from genuine same-sign lepton pairs (WZ, ZZ, leptons from same-sign W from single-, double-parton, and $t\bar{t}W$ production, etc.), as well as electrons from converted photons in $V\gamma$ production. Entries with zero contributing events are reported with an uncertainty corresponding to one event. This uncertainty is not added to the total MC contribution. Systematic uncertainties (the second uncertainty if present) are displayed only for the final combined type of background, no systematic uncertainty is added for estimates with zero entries. Systematic uncertainties are 100% correlated among the channels.

17

The estimation is in a good agreement with the observation. We also note that the backgrounds with respect to the inclusive same-sign dilepton search is suppressed by an order of magnitude due to the b-tag requirements.

We have visually scanned all the events in data and provide details in Section 8.

7.1 Discussion of Background Expectation From MC

THIS SECTION NEEDS TO BE UPDATED

Three MC studies are presented. First, we show the origin of fake leptons in MC. Second, we show explicitly the degree to which the fake rate method accurately predicts the fake lepton background in $t\bar{t}$ MC, and third, we present evidence for our assertion that a b-quark can not simultaneously provide a b-tag and produce a fake lepton.

We use a large $t\bar{t}$ sample [1] normalized to 1 fb^{-1} for these studies. The fake rates were obtained from QCD MC as described in detail in [3].

We classify $t\bar{t}$ background events based on truth matching to their "parent parton" as either "Heavy Flavor" or "Light Flavor". Charm quarks from W decay are classified as heavy flavor. It is thus possible to have three heavy quarks in the same event, one of which provides the isolated lepton, the two others the b-tags.

As is shown in Table 14 about 60% (40%) of the fake leptons are from heavy (light) flavor.

Same Sign Leptons	Total	Heavy Flavor	Light Flavor
ee	0.31±0.07	0.11±0.04	0.21±0.05
$\mu\mu$	0.26±0.06	0.22±0.05	0.04±0.04
$e\mu$	0.57±0.09	0.37±0.07	0.21±0.05
total	1.15±0.13	0.70±0.10	0.45± 0.08

Table 14: Expected number of $t\bar{t}$ events in 1 fb^{-1} of integrated luminosity. Uncertainties are from MC statistics.

Table 15 shows the same breakdown for the fake rate prediction. Here we use an MC sample where one of the W's is forced to decay leptonically while the other is not allowed to decay leptonically. We use this sample as it has x10 the luminosity equivalent than the standard $t\bar{t}$ sample, thus providing higher statistics for this test. We observe an overprediction of 30% which appears to be primarily due to overpredicting the fakes from heavy flavor.

Same Sign Leptons	Total	Heavy Flavor	Light Flavor
ee	0.39±0.03	0.20±0.02	0.19±0.03
$\mu\mu$	0.36±0.03	0.30±0.03	0.06±0.01
$e\mu$	0.76±0.05	0.54±0.04	0.22±0.03
total	1.51±0.06	1.04±0.05	0.47±0.04

Table 15: Predicted number of $t\bar{t}$ events in 1 fb^{-1} of integrated luminosity. Uncertainties are from MC statistics.

Finally, Figure 7 shows the minimum ΔR between one of the two b-tagged jets and the fake lepton in the MC after relaxing the jet veto cone around the lepton. The black line indicates the jet veto cone size. Clearly, a b-quark can not simultaneously provide a b-tag and an isolated lepton.

8 Results on Inlcusive Signature Search

This section is missing two things. First, we will add a $\not{E}_T$ vs H_T plot that shows the data and one of the models overlayed. Second, we will add a summary of the events we see.

We see 2 (1) events in the high-p_T (low-p_T) analysis with a predicted background of 1.0± 0.8 (0.5± 0.7). In absence of any significant deviation from the predicted background, we set 95% CL. on the number of observed events. Two statistical methods have been used for the upper limit. Both methods assume the uncertainties on signal and background are un-correlated and use a log-normal distribution for error pdfs.

The first method used to compute the upper limit is based on the Bayesian method [8]. A posterior probability $p(r)$ is used as a function of the signal strength $r = \sigma/\sigma_{SM}$ assuming a uniform prior for the signal strength r

---

[1] The POWHEG sample TTToLNu2Q2B_7TeV-powheg-pythia6_Spring11-PU_S1_START311_V1G1-v1
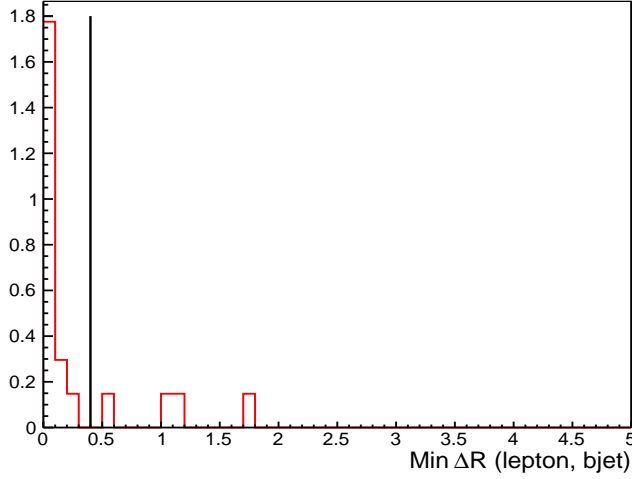
18

Figure 7: Minimum ΔR between the lepton and the b-tag jet in $t\bar{t}$ decays.

integrating the nuisance parameters associated with the uncertainties. The upper limit at 95% confidence level is then determined by integrating $p(r)$ to determine r', which satisfies $\int_{r'}^{\inf} p(r)dr = 0.05$.

We use the hybrid frequentist-bayesian CLs approach [7] as the second method. Although the two statistical approaches are not equivalent, in this case we get similar results.

- Upper limit using high-p_T analysis at 95% CL. with 24% signal systematic error using Bayesian approach = 6.1

- Upper limit using high-p_T analysis at 95% CL. with 24% signal systematic error using CLs = 5.8

- Upper limit using low-p_T analysis at 95% CL. with 24% signal systematic error using Bayesian approach = 4.8

- Upper limit using low-p_T analysis at 95% CL. with 24% signal systematic error using CLs = 4.6

We use 6.1 and 4.8 events as the upper limit for the rest of this document for high- and low-p_T analyses.

9 Searches for Specific Models

Our signature, two isolated same-sign leptons plus, at least two b-tagged jets, and $\not{E}_T$, is common to many different new physics scenarios, as well as standard model $t\bar{t}W$ production.

Here we refine our analysis to define dedicated signal regions for a few of these scenarios, and provide 95% C.L. upper limits on their respective model parameter space.

We expect to explore the following models for the final paper:

- Top pair production via t-channel Z' exchange as proposed by [11] and searched for by CMS with 2010 data [1]. This is in some ways a minimal model for our purposes, as it produces nothing other than same sign dileptons, two b-jets, and moderate $\not{E}_T$ typical for two leptonic W decays.

- A simplified model for same-sing top pair production as suggested in [13]. The production mechanisms here range from t-channel uu-scattering to tt, as in the previous example, to $tt\bar{u}\bar{u}$. The main difference to the previous model is different kinematics of the top quarks due to an intermediate resonance $\eta^0 \to t\bar{u}$ decay. The mass of the η^0 is the main parameter in the simplified model.

- Standard model $t\bar{t}W$ production. Here the final state is same sign dileptons, two neutrinos, i.e. moderate $\not{E}_T$, plus one top quark that decays generically.

- $T_{5/3}$ fermion from Little Higgs models as suggested in [12] lead to a $t\bar{t}W^+W^-$ final state, thus providing one additional W over the previous example.

19

- SUSY gluino pair production with the gluino decaying to top and stop as suggested in [9][10]. Depending on stop mass, this leads to a final state of either $t\bar{t}t\bar{t}$ plus $\not{E}_T$, or $tt\bar{Q}\bar{Q}$ plus $\not{E}_T$ with Q being charm or beauty, and charge conjugates, as sources for the same sign dilepton plus two btags plus $\not{E}_T$. Independent of stop mass, final states with same sign dileptons plus four heavy flavor quarks plus $\not{E}_T$ are produced.

We will fill this in as we generate the samples, and figure out what minor changes to our baseline cuts each model requires to be sort of moderately optimized. In general, we expect changes in lepton p_T, $\not{E}_T$, H_T, and possibly jet p_T requirements, but no object selection changes.

Below are some other ideas being tossed around for other analyses, that we might be competitive with in some parts of the parameter space.

- Pair production of heavy flavored squarks and their anti-squarks [14]. In its simplest form, this just gives $t\bar{t}$ plus $\not{E}_T$, $t\bar{b}$ plus $\not{E}_T$, or $b\bar{b}$ plus $\not{E}_T$, and is thus not relevant for us. It's being looked at in the context of the $\not{E}_T$ plus jets analyses. However, there is a variant for which the stop decay proceeds through an intermediate neutralino that decays to W plus chargino, with the chargino being close to degenerate in mass with the neutralino LSP. In this case, the stop anti-stop production mechanism results in a $t\bar{t}W^+W^-$ plus $\not{E}_T$ final state. This is thus the same final state as the $T_{5/3}$ pair production mentioned above, except with two additional LSPs. There may be parts of the parameter space for which the LSP is very light, thus not providing enough $\not{E}_T$ for the $\not{E}_T$ plus jets analyses to see it, or the opposite extreme, where the LSP is so massive, that the Q value of the decays leads to LSPs at rest in the labframe, and thus little $\not{E}_T$. Not sure to what extend these corners of phase space are big enough to pursue.

- Pair production of color octet neutral scalars that each decay to $t\bar{t}$ [15], thus leading to a final state similar as the the SUSY gluino pair production, except with no additional $\not{E}_T$ beyond the neutrinos from leptonic W decay. This might thus be possibly missed by the usual $\not{E}_T$ plus jets analyses because it doesn't have enough $\not{E}_T$. It might be a target for us more than them.

10 Conclusion

In conclusion, the first search using same-sign dileptons with b-jets and $\not{E}_T$ has been presented. In the proton-proton collision data sample corresponding to an integrated luminosity of 349 pb^{-1} at $\sqrt{s}$ = 7 TeV, no significant deviations from the Standard Model expectations are observed. We use this data to set 95% CL. on the number of observed events.

References

[1] S. Chatrchyan *et al.* [CMS Collaboration], *"Search for Same-Sign Top-Quark Pair Production at $\sqrt{s} = 7$ TeV and Limits on Flavour Changing Neutral Currents in the Top Sector,"* JHEP **1108**, 005 (2011) [arXiv:1106.2142 [hep-ex]].

[2] S. Chatrchyan *et al.* [CMS Collaboration], *"Search for new physics with same-sign isolated dilepton events with jets and missing transverse energy at the LHC,"* JHEP **1106**, 077 (2011) [arXiv:1104.3168 [hep-ex]].

[3] *"Search for New Physics with Same-Sign dileptons using the 2011 dataset of CMS"*, CMS AN-2011/468.

[4] CMS Collaboration, *"Search for new physics with same-sign isolated dilepton events with jets and missing energy"*, CMS PAS SUS-11-010/SUS-11-025, in preparation.

[5] CMS Collaboration, *"Measurement from data of efficiency and mistag rate of b-tagging algorithms using 2010 data"*, PAS BTV-11-001 (Submitted)

[6] *"Fake Rates for Dilepton Analyses"*, CMS AN-2010/257.

[7] A.L. Read, CERN Report 2000-005 p. 81 (2000).

[8] whatever, some bayesian reference.

[9] http://arxiv.org/abs/hep-ph/0512284,SUSY Gluinos to light stop

[10] http://arxiv.org/abs/1004.2256,more SUSY Gluinos to light stop

[11] The same sign top, E. Berger et al.

[12] http://arxiv.org/abs/0801.1679, $T_{5/3}$ fermion pair production leading to $t\bar{t}W^{+}W^{-}$ final state.

[13] http://lhcnewphysics.org/l.006.00.r000, Simplified model by Felix Yu, UCI

[14] http://lhcnewphysics.org/b.011.00.r000 , Stop anti-stop production proposal by Toro et al.

[15] http://lhcnewphysics.org/b.007.00.r000 , $t\bar{t}t\bar{t}$ production via pair production of a neutral color octet resonance by Toro et al.

[16] A. G. Cohen, D. B. Kaplan and A. E. Nelson, *"The More minimal supersymmetric standard model,"* Phys. Lett. B **388**, 588 (1996) [hep-ph/9607394].

[17] S. Dimopoulos and G. F. Giudice, *"Naturalness constraints in supersymmetric theories with nonuniversal soft terms,"* Phys. Lett. B **357**, 573 (1995) [hep-ph/9507282].

[18] R. Barbieri, G. R. Dvali and L. J. Hall, *"Predictions from a U(2) flavor symmetry in supersymmetric theories,"* Phys. Lett. B **377**, 76 (1996) [hep-ph/9512388].

[19] M. Papucci, J. T. Ruderman and A. Weiler, *"Natural SUSY Endures,"* arXiv:1110.6926 [hep-ph].

[20] B. S. Acharya, P. Grajek, G. L. Kane, E. Kuflik, K. Suruliz and L. -T. Wang, *"Identifying Multi-Top Events from Gluino Decay at the LHC,"* arXiv:0901.3367 [hep-ph].

[21] G. L. Kane, E. Kuflik, R. Lu and L. -T. Wang, *"Top Channel for Early SUSY Discovery at the LHC,"* Phys. Rev. D **84**, 095004 (2011) [arXiv:1101.1963 [hep-ph]].

[22] S. Kraml and A. R. Raklev, *"Same-sign top quarks as signature of light stops at the LHC,"* Phys. Rev. D **73**, 075002 (2006) [hep-ph/0512284].

[23] R. Essig, E. Izaguirre, J. Kaplan and J. G. Wacker, *"Heavy Flavor Simplified Models at the LHC,"* arXiv:1110.6443 [hep-ph].

[24] T. Plehn and T. M. P. Tait, *"Seeking Sgluons,"* J. Phys. G G **36**, 075001 (2009) [arXiv:0810.3919 [hep-ph]].

[25] M. Gerbush, T. J. Khoo, D. J. Phalen, A. Pierce and D. Tucker-Smith, *"Color-octet scalars at the CERN LHC,"* Phys. Rev. D **77**, 095003 (2008) [arXiv:0710.3133 [hep-ph]].

[26] S. Bar-Shalom and A. Rajaraman, *"Models and phenomenology of maximal flavor violation,"* Phys. Rev. D **77**, 095011 (2008) [arXiv:0711.3193 [hep-ph]].

[27] S. Bar-Shalom, A. Rajaraman, D. Whiteson and F. Yu, *"Collider Signals of Maximal Flavor Violation: Same-Sign Leptons from Same-Sign Tops at the Tevatron,"* Phys. Rev. D **78**, 033003 (2008) [arXiv:0803.3795 [hep-ph]].

[28] T. Aaltonen *et al.* [CDF Collaboration], *"Search for Maximal Flavor Violating Scalars in Same-Charge Lepton Pairs in $p\bar{p}$ Collisions at $\sqrt{s}$ = 1.96-TeV,"* Phys. Rev. Lett. **102**, 041801 (2009) [arXiv:0809.4903 [hep-ex]].

[29] R. Contino and G. Servant, *"Discovering the top partners at the LHC using same-sign dilepton final states,"* JHEP **0806**, 026 (2008) [arXiv:0801.1679 [hep-ph]].

[30] B. Lillie, J. Shu and T. M. P. Tait, *"Top Compositeness at the Tevatron and LHC,"* JHEP **0804**, 087 (2008) [arXiv:0712.3057 [hep-ph]].

[31] A. Pomarol and J. Serra, *"Top Quark Compositeness: Feasibility and Implications,"* Phys. Rev. D **78**, 074026 (2008) [arXiv:0806.3247 [hep-ph]].

[32] K. Kumar, T. M. P. Tait and R. Vega-Morales, *"Manifestations of Top Compositeness at Colliders,"* JHEP **0905**, 022 (2009) [arXiv:0901.3808 [hep-ph]].

[33] E. L. Berger, Q. -H. Cao, C. -R. Chen, C. S. Li and H. Zhang, *"Top Quark Forward-Backward Asymmetry and Same-Sign Top Quark Pairs,"* Phys. Rev. Lett. **106**, 201801 (2011) [arXiv:1101.5625 [hep-ph]].

[34] CMS Collaboration, *"Measurement of the b-tagging efficiency using $t\bar{t}$ events"*, PAS BTV-11-003, in preparation.

[35] M. Narain for BTV POG, `https://indico.cern.ch/getFile.py/access?contribId=0&resId=1&materialId=slides&confId=163892`

22

A   Results - Exclusive Yields

In the following we report yields of events observed in data and compare them to the predictions from the data-driven methods as well as from simulation. These results are reported for *high-p_T* and *low-p_T* dilepton selections with H_T and $\not{E}_T$ selected as defined in the baseline selection described in Section **??**, as well as for the signal regions defined in Section **??**. As anticipated, the MC predicts that $t\bar{t}$ is the largest background in all cases. The data yield is in good agreement with the prediction from both MC as well as the data driven prediction. The procedure for arriving at these data driven predictions is detailed in Section 5. These data-driven predictions supersede all the MC estimates of the contributions from events with fake leptons or with leptons with misreconstructed charge. The remaining MC contribution in the final estimates of background events are those with real leptons: $WZ \rightarrow lll\nu$, $ZZ \rightarrow llll$; same-sign W from single-parton (spWW), double-parton (dpWW), and $t\bar{t}W$ production. Note that we have also included a contribution from W/Z+γ background events where the asymmetric conversion of the photon can give rise to an electron of the same sign as a lepton from W or Z. This background is not predicted by the fake lepton prediction method. Results of background estimates in simulation and data are compared with the number of observed events in data in the tables below. The SUSY LM2 point yield based on the LO cross section is provided as a reference. The NLO/LO k-factor for LM2 is 1.33 [**?**].

Source	ee	$\mu\mu$	eμ	all
$t\bar{t} \to \ell\ell X$	0.071 ± 0.199	0.000 ± 0.199	0.000 ± 0.199	0.071 ± 0.199
$t\bar{t}$ other	0.000 ± 0.199	0.000 ± 0.199	0.000 ± 0.199	0.000 ± 0.199
$t\bar{t} \to \ell(b \to \ell)X$	0.000 ± 0.199	0.000 ± 0.199	0.000 ± 0.199	0.000 ± 0.199
$t\bar{t} \to \ell(\not{b} \to \ell)X$	0.000 ± 0.199	0.000 ± 0.199	0.130 ± 0.130	0.130 ± 0.130
t, s-channel	0.000 ± 0.057	0.000 ± 0.057	0.000 ± 0.057	0.000 ± 0.057
t, t-channel	0.000 ± 0.055	0.000 ± 0.055	0.000 ± 0.055	0.000 ± 0.055
tW	0.000 ± 0.045	0.000 ± 0.045	0.000 ± 0.045	0.000 ± 0.045
$Z \to ee$	0.000 ± 0.429	0.000 ± 0.429	0.000 ± 0.429	0.000 ± 0.429
$Z \to \mu\mu$	0.000 ± 0.429	0.000 ± 0.429	0.000 ± 0.429	0.000 ± 0.429
$Z \to \tau\tau$	0.000 ± 0.429	0.000 ± 0.429	0.000 ± 0.429	0.000 ± 0.429
W+jets	0.000 ± 1.808	0.000 ± 1.808	0.000 ± 1.808	0.000 ± 1.808
WW	0.000 ± 0.019	0.000 ± 0.019	0.000 ± 0.019	0.000 ± 0.019
$V\gamma$	0.000 ± 0.248	0.000 ± 0.248	0.000 ± 0.248	0.000 ± 0.248
$W\gamma^* \to \ell\nu ee$	0.000 ± 0.097	0.000 ± 0.097	0.000 ± 0.097	0.000 ± 0.097
$W\gamma^* \to \ell\nu\mu\mu$	0.000 ± 0.075	0.000 ± 0.075	0.000 ± 0.075	0.000 ± 0.075
$W\gamma^* \to \ell\nu\tau\tau$	0.000 ± 0.028	0.000 ± 0.028	0.000 ± 0.028	0.000 ± 0.028
WZ	0.005 ± 0.005	0.000 ± 0.003	0.002 ± 0.002	0.007 ± 0.005
ZZ	0.000 ± 0.000	0.000 ± 0.000	0.000 ± 0.000	0.000 ± 0.000
$dpW^{\pm}W^{\pm}$	0.000 ± 0.004	0.000 ± 0.004	0.000 ± 0.004	0.000 ± 0.004
spW^-W^-	0.000 ± 0.001	0.000 ± 0.001	0.000 ± 0.001	0.000 ± 0.001
spW^+W^+	0.000 ± 0.006	0.000 ± 0.006	0.000 ± 0.006	0.000 ± 0.006
$t\bar{t}\gamma$	0.000 ± 0.059	0.000 ± 0.059	0.000 ± 0.059	0.000 ± 0.059
$t\bar{t}W$	0.073 ± 0.009	0.077 ± 0.009	0.145 ± 0.013	0.295 ± 0.018
$t\bar{t}Z$	0.012 ± 0.003	0.021 ± 0.004	0.032 ± 0.005	0.065 ± 0.007
$WW\gamma$	0.000 ± 0.015	0.000 ± 0.015	0.000 ± 0.015	0.000 ± 0.015
WWW	0.000 ± 0.000	0.000 ± 0.000	0.000 ± 0.000	0.000 ± 0.000
WWZ	0.000 ± 0.000	0.000 ± 0.000	0.000 ± 0.000	0.000 ± 0.000
WZZ	0.000 ± 0.000	0.000 ± 0.000	0.000 ± 0.000	0.000 ± 0.000
ZZZ	0.000 ± 0.000	0.000 ± 0.000	0.000 ± 0.000	0.000 ± 0.000
Total MC	0.160 ± 0.072	0.099 ± 0.010	0.309 ± 0.131	0.568 ± 0.150
LM6	0.000 ± 0.000	0.000 ± 0.000	0.000 ± 0.000	0.000 ± 0.000
SF	0.27 ± 0.54	0.00 ± 0.37	0.39 ± 0.57	0.66 ± 0.72
DF	0.00 ± 0.14	0.00 ± 0.10	0.00 ± 0.16	0.00 ± 0.16
SF + DF	$0.27 \pm 0.45 \pm 0.14$	$0.00 \pm 0.31 \pm 0.00$	$0.39 \pm 0.47 \pm 0.19$	$0.66 \pm 0.65 \pm 0.33$
Charge Flips	$0.016 \pm 0.007 \pm 0.003$	$- \pm -$	$0.047 \pm 0.010 \pm 0.009$	$0.063 \pm 0.012 \pm 0.013$
MC Pred	$0.089 \pm 0.011 \pm 0.045$	$0.099 \pm 0.010 \pm 0.049$	$0.179 \pm 0.014 \pm 0.090$	$0.367 \pm 0.020 \pm 0.183$
Total Pred	$0.378 \pm 0.453 \pm 0.144$	$0.099 \pm 0.315 \pm 0.049$	$0.612 \pm 0.470 \pm 0.213$	$1.089 \pm 0.653 \pm 0.377$
data	0	1	0	1

Table 16: Observed event yields in high-p_T (pT > 20/10) dileptons passing the *low-m_0* signal selections ($320 < H_T < 440$ GeV, $50 < \not{E}_T < 120$ GeV) compared to expectations from simulation alone, and from the data-driven methods. The *simulated backgrounds* contribution includes contributions from genuine same-sign lepton pairs (WZ, ZZ, leptons from same-sign W from single-, double-parton, and $t\bar{t}W$ production), as well as electrons from converted photons in $V\gamma$ production. Entries with zero contributing events are reported with an uncertainty corresponding to one event. This uncertainty is not added to the total MC contribution. Systematic uncertainties (the second uncertainty if present) are displayed only for the final combined type of background, no systematic uncertainty is added for estimates with zero entries. Systematic uncertainties are 100% correlated among the channels.

Source	ee	$\mu\mu$	eμ	all
$t\bar{t} \to \ell\ell X$	0.000 ± 0.199	0.000 ± 0.199	0.000 ± 0.199	0.000 ± 0.199
$t\bar{t}$ other	0.000 ± 0.199	0.000 ± 0.199	0.000 ± 0.199	0.000 ± 0.199
$t\bar{t} \to \ell(b \to \ell)X$	0.000 ± 0.199	0.000 ± 0.199	0.000 ± 0.199	0.000 ± 0.199
$t\bar{t} \to \ell(\bar{b} \to \ell)X$	0.272 ± 0.272	0.000 ± 0.199	0.000 ± 0.199	0.272 ± 0.272
t, s-channel	0.000 ± 0.057	0.000 ± 0.057	0.000 ± 0.057	0.000 ± 0.057
t, t-channel	0.000 ± 0.055	0.000 ± 0.055	0.000 ± 0.055	0.000 ± 0.055
tW	0.000 ± 0.045	0.000 ± 0.045	0.000 ± 0.045	0.000 ± 0.045
$Z \to ee$	0.000 ± 0.429	0.000 ± 0.429	0.000 ± 0.429	0.000 ± 0.429
$Z \to \mu\mu$	0.000 ± 0.429	0.000 ± 0.429	0.000 ± 0.429	0.000 ± 0.429
$Z \to \tau\tau$	0.000 ± 0.429	0.000 ± 0.429	0.000 ± 0.429	0.000 ± 0.429
W+jets	0.000 ± 1.808	0.000 ± 1.808	0.000 ± 1.808	0.000 ± 1.808
WW	0.000 ± 0.019	0.000 ± 0.019	0.000 ± 0.019	0.000 ± 0.019
Vγ	0.000 ± 0.248	0.000 ± 0.248	0.000 ± 0.248	0.000 ± 0.248
$W\gamma^* \to \ell\nu ee$	0.000 ± 0.097	0.000 ± 0.097	0.000 ± 0.097	0.000 ± 0.097
$W\gamma^* \to \ell\nu\mu\mu$	0.000 ± 0.075	0.000 ± 0.075	0.000 ± 0.075	0.000 ± 0.075
$W\gamma^* \to \ell\nu\tau\tau$	0.000 ± 0.028	0.000 ± 0.028	0.000 ± 0.028	0.000 ± 0.028
WZ	0.000 ± 0.003	0.001 ± 0.003	0.004 ± 0.004	0.005 ± 0.004
ZZ	0.000 ± 0.000	0.000 ± 0.000	0.000 ± 0.000	0.000 ± 0.000
dp$W^{\pm}W^{\pm}$	0.000 ± 0.004	0.000 ± 0.004	0.000 ± 0.004	0.000 ± 0.004
spW^-W^-	0.000 ± 0.001	0.000 ± 0.001	0.001 ± 0.001	0.001 ± 0.001
spW^+W^+	0.000 ± 0.006	0.000 ± 0.006	0.000 ± 0.006	0.000 ± 0.006
$t\bar{t}\gamma$	0.000 ± 0.059	0.000 ± 0.059	0.000 ± 0.059	0.000 ± 0.059
$t\bar{t}W$	0.099 ± 0.011	0.097 ± 0.010	0.184 ± 0.014	0.379 ± 0.020
$t\bar{t}Z$	0.020 ± 0.004	0.028 ± 0.004	0.049 ± 0.005	0.098 ± 0.008
$WW\gamma$	0.000 ± 0.015	0.000 ± 0.015	0.000 ± 0.015	0.000 ± 0.015
WWW	0.000 ± 0.000	0.000 ± 0.000	0.000 ± 0.000	0.001 ± 0.001
WWZ	0.000 ± 0.000	0.000 ± 0.000	0.000 ± 0.000	0.000 ± 0.000
WZZ	0.000 ± 0.000	0.000 ± 0.000	0.000 ± 0.000	0.000 ± 0.000
ZZZ	0.000 ± 0.000	0.000 ± 0.000	0.000 ± 0.000	0.000 ± 0.000
Total MC	0.391 ± 0.272	0.126 ± 0.011	0.239 ± 0.015	0.756 ± 0.273
LM6	0.000 ± 0.000	0.186 ± 0.186	0.383 ± 0.275	0.569 ± 0.332
SF	0.00 ± 0.58	0.00 ± 0.37	0.15 ± 0.54	0.15 ± 0.54
DF	0.00 ± 0.14	0.00 ± 0.10	0.00 ± 0.16	0.00 ± 0.16
SF + DF	$0.00 \pm 0.50 \pm 0.00$	$0.00 \pm 0.31 \pm 0.00$	$0.15 \pm 0.44 \pm 0.07$	$0.15 \pm 0.44 \pm 0.07$
Charge Flips	$0.011 \pm 0.004 \pm 0.002$	$- \pm -$	$0.016 \pm 0.005 \pm 0.003$	$0.027 \pm 0.006 \pm 0.005$
MC Pred	$0.119 \pm 0.011 \pm 0.060$	$0.126 \pm 0.011 \pm 0.063$	$0.239 \pm 0.015 \pm 0.119$	$0.485 \pm 0.022 \pm 0.242$
Total Pred	$0.130 \pm 0.501 \pm 0.060$	$0.126 \pm 0.315 \pm 0.063$	$0.404 \pm 0.438 \pm 0.141$	$0.661 \pm 0.438 \pm 0.254$
data	1	0	0	1

Table 17: Observed event yields in high-p_T (pT > 20/10) dileptons passing the *high-m$_0$* signal selections ($H_T >$ 440 GeV, $\not{E}_T >$ 50 GeV) compared to expectations from simulation alone, and from the data-driven methods. The *simulated backgrounds* contribution includes contributions from genuine same-sign lepton pairs (WZ, ZZ, leptons from same-sign W from single-, double-parton, and $t\bar{t}W$ production), as well as electrons from converted photons in $V\gamma$ production. Entries with zero contributing events are reported with an uncertainty corresponding to one event. This uncertainty is not added to the total MC contribution. Systematic uncertainties (the second uncertainty if present) are displayed only for the final combined type of background, no systematic uncertainty is added for estimates with zero entries. Systematic uncertainties are 100% correlated among the channels.

Source	ee	$\mu\mu$	eμ	all
$t\bar{t} \to \ell\ell X$	0.000 ± 0.199	0.000 ± 0.199	0.000 ± 0.199	0.000 ± 0.199
$t\bar{t}$ other	0.000 ± 0.199	0.000 ± 0.199	0.000 ± 0.199	0.000 ± 0.199
$t\bar{t} \to \ell(b \to \ell)X$	0.000 ± 0.199	0.000 ± 0.199	0.000 ± 0.199	0.000 ± 0.199
$t\bar{t} \to \ell(\bar{b} \to \ell)X$	0.000 ± 0.199	0.000 ± 0.199	0.000 ± 0.199	0.000 ± 0.199
t, s-channel	0.000 ± 0.057	0.000 ± 0.057	0.000 ± 0.057	0.000 ± 0.057
t, t-channel	0.000 ± 0.055	0.000 ± 0.055	0.000 ± 0.055	0.000 ± 0.055
tW	0.000 ± 0.045	0.000 ± 0.045	0.000 ± 0.045	0.000 ± 0.045
$Z \to ee$	0.000 ± 0.429	0.000 ± 0.429	0.000 ± 0.429	0.000 ± 0.429
$Z \to \mu\mu$	0.000 ± 0.429	0.000 ± 0.429	0.000 ± 0.429	0.000 ± 0.429
$Z \to \tau\tau$	0.000 ± 0.429	0.000 ± 0.429	0.000 ± 0.429	0.000 ± 0.429
W+jets	0.000 ± 1.808	0.000 ± 1.808	0.000 ± 1.808	0.000 ± 1.808
WW	0.000 ± 0.019	0.000 ± 0.019	0.000 ± 0.019	0.000 ± 0.019
$V\gamma$	0.000 ± 0.248	0.000 ± 0.248	0.000 ± 0.248	0.000 ± 0.248
$W\gamma^* \to \ell\nu ee$	0.000 ± 0.097	0.000 ± 0.097	0.000 ± 0.097	0.000 ± 0.097
$W\gamma^* \to \ell\nu\mu\mu$	0.000 ± 0.075	0.000 ± 0.075	0.000 ± 0.075	0.000 ± 0.075
$W\gamma^* \to \ell\nu\tau\tau$	0.000 ± 0.028	0.000 ± 0.028	0.000 ± 0.028	0.000 ± 0.028
WZ	0.005 ± 0.005	0.000 ± 0.003	0.000 ± 0.003	0.005 ± 0.005
ZZ	0.000 ± 0.000	0.000 ± 0.000	0.000 ± 0.000	0.000 ± 0.000
$dpW^{\pm}W^{\pm}$	0.000 ± 0.004	0.000 ± 0.004	0.000 ± 0.004	0.000 ± 0.004
spW^-W^-	0.000 ± 0.001	0.000 ± 0.001	0.000 ± 0.001	0.000 ± 0.001
spW^+W^+	0.000 ± 0.006	0.000 ± 0.006	0.000 ± 0.006	0.000 ± 0.006
$t\bar{t}\gamma$	0.000 ± 0.059	0.000 ± 0.059	0.000 ± 0.059	0.000 ± 0.059
$t\bar{t}W$	0.028 ± 0.006	0.041 ± 0.006	0.076 ± 0.009	0.145 ± 0.012
$t\bar{t}Z$	0.003 ± 0.001	0.009 ± 0.003	0.008 ± 0.002	0.020 ± 0.004
$WW\gamma$	0.000 ± 0.015	0.000 ± 0.015	0.000 ± 0.015	0.000 ± 0.015
WWW	0.000 ± 0.000	0.000 ± 0.000	0.000 ± 0.000	0.000 ± 0.000
WWZ	0.000 ± 0.000	0.000 ± 0.000	0.000 ± 0.000	0.000 ± 0.000
WZZ	0.000 ± 0.000	0.000 ± 0.000	0.000 ± 0.000	0.000 ± 0.000
ZZZ	0.000 ± 0.000	0.000 ± 0.000	0.000 ± 0.000	0.000 ± 0.000
Total MC	0.036 ± 0.008	0.049 ± 0.007	0.085 ± 0.009	0.170 ± 0.014
LM6	0.000 ± 0.000	0.000 ± 0.000	0.000 ± 0.000	0.000 ± 0.000
SF	0.00 ± 0.58	0.00 ± 0.37	0.18 ± 0.55	0.18 ± 0.55
DF	0.00 ± 0.14	0.00 ± 0.10	0.00 ± 0.16	0.00 ± 0.16
SF + DF	$0.00 \pm 0.50 \pm 0.00$	$0.00 \pm 0.31 \pm 0.00$	$0.18 \pm 0.45 \pm 0.09$	$0.18 \pm 0.45 \pm 0.09$
Charge Flips	$0.007 \pm 0.003 \pm 0.001$	$- \pm -$	$0.010 \pm 0.004 \pm 0.002$	$0.017 \pm 0.005 \pm 0.003$
MC Pred	$0.036 \pm 0.008 \pm 0.018$	$0.049 \pm 0.007 \pm 0.025$	$0.085 \pm 0.009 \pm 0.042$	$0.170 \pm 0.014 \pm 0.085$
Total Pred	$0.043 \pm 0.501 \pm 0.018$	$0.049 \pm 0.315 \pm 0.025$	$0.270 \pm 0.447 \pm 0.097$	$0.363 \pm 0.447 \pm 0.122$
data	1	0	1	2

Table 18: Observed event yields in high-p_T (pT > 20/10) dileptons passing the *simplified model* signal selections ($200 < H_T < 320$ GeV, $\not{E}_T > 120$ GeV) compared to expectations from simulation alone, and from the data-driven methods. The *simulated backgrounds* contribution includes contributions from genuine same-sign lepton pairs (WZ, ZZ, leptons from same-sign W from single-, double-parton, and $t\bar{t}W$ production), as well as electrons from converted photons in $V\gamma$ production. Entries with zero contributing events are reported with an uncertainty corresponding to one event. This uncertainty is not added to the total MC contribution. Systematic uncertainties (the second uncertainty if present) are displayed only for the final combined type of background, no systematic uncertainty is added for estimates with zero entries. Systematic uncertainties are 100% correlated among the channels.

Source	ee	$\mu\mu$	eμ	all
$t\bar{t} \to \ell\ell X$	0.000 ± 0.199	0.000 ± 0.199	0.000 ± 0.199	0.000 ± 0.199
$t\bar{t}$ other	0.000 ± 0.199	0.000 ± 0.199	0.000 ± 0.199	0.000 ± 0.199
$t\bar{t} \to \ell(b \to \ell)X$	0.000 ± 0.199	0.000 ± 0.199	0.000 ± 0.199	0.000 ± 0.199
$t\bar{t} \to \ell(\bar{b} \to \ell)X$	0.000 ± 0.199	0.000 ± 0.199	0.000 ± 0.199	0.000 ± 0.199
t, s-channel	0.000 ± 0.057	0.000 ± 0.057	0.000 ± 0.057	0.000 ± 0.057
t, t-channel	0.000 ± 0.055	0.000 ± 0.055	0.000 ± 0.055	0.000 ± 0.055
tW	0.000 ± 0.045	0.000 ± 0.045	0.000 ± 0.045	0.000 ± 0.045
$Z \to ee$	0.000 ± 0.429	0.000 ± 0.429	0.000 ± 0.429	0.000 ± 0.429
$Z \to \mu\mu$	0.000 ± 0.429	0.000 ± 0.429	0.000 ± 0.429	0.000 ± 0.429
$Z \to \tau\tau$	0.000 ± 0.429	0.000 ± 0.429	0.000 ± 0.429	0.000 ± 0.429
W+jets	0.000 ± 1.808	0.000 ± 1.808	0.000 ± 1.808	0.000 ± 1.808
WW	0.000 ± 0.019	0.000 ± 0.019	0.000 ± 0.019	0.000 ± 0.019
Vγ	0.000 ± 0.248	0.000 ± 0.248	0.000 ± 0.248	0.000 ± 0.248
$W\gamma^* \to \ell\nu ee$	0.000 ± 0.097	0.000 ± 0.097	0.000 ± 0.097	0.000 ± 0.097
$W\gamma^* \to \ell\nu \mu\mu$	0.000 ± 0.075	0.000 ± 0.075	0.000 ± 0.075	0.000 ± 0.075
$W\gamma^* \to \ell\nu \tau\tau$	0.000 ± 0.028	0.000 ± 0.028	0.000 ± 0.028	0.000 ± 0.028
WZ	0.004 ± 0.004	0.001 ± 0.003	0.000 ± 0.003	0.006 ± 0.005
ZZ	0.000 ± 0.000	0.000 ± 0.000	0.000 ± 0.000	0.000 ± 0.000
dp$W^{\pm}W^{\pm}$	0.000 ± 0.004	0.000 ± 0.004	0.000 ± 0.004	0.000 ± 0.004
spW^-W^-	0.000 ± 0.001	0.000 ± 0.001	0.001 ± 0.001	0.001 ± 0.001
spW^+W^+	0.000 ± 0.006	0.000 ± 0.006	0.000 ± 0.006	0.000 ± 0.006
$t\bar{t}\gamma$	0.000 ± 0.059	0.000 ± 0.059	0.000 ± 0.059	0.000 ± 0.059
$t\bar{t}W$	0.069 ± 0.009	0.080 ± 0.009	0.168 ± 0.013	0.317 ± 0.018
$t\bar{t}Z$	0.013 ± 0.003	0.014 ± 0.003	0.033 ± 0.005	0.060 ± 0.006
$WW\gamma$	0.000 ± 0.015	0.000 ± 0.015	0.000 ± 0.015	0.000 ± 0.015
WWW	0.000 ± 0.000	0.000 ± 0.000	0.000 ± 0.000	0.001 ± 0.000
WWZ	0.000 ± 0.000	0.000 ± 0.000	0.000 ± 0.000	0.000 ± 0.000
WZZ	0.000 ± 0.000	0.000 ± 0.000	0.000 ± 0.000	0.000 ± 0.000
ZZZ	0.000 ± 0.000	0.000 ± 0.000	0.000 ± 0.000	0.000 ± 0.000
Total MC	0.086 ± 0.010	0.096 ± 0.010	0.203 ± 0.014	0.385 ± 0.020
LM6	0.000 ± 0.000	0.186 ± 0.186	0.383 ± 0.275	0.569 ± 0.332
SF	0.00 ± 0.58	0.00 ± 0.37	0.15 ± 0.54	0.15 ± 0.54
DF	0.00 ± 0.14	0.00 ± 0.10	0.00 ± 0.16	0.00 ± 0.16
SF + DF	0.00 ± 0.50 ± 0.00	0.00 ± 0.31 ± 0.00	0.15 ± 0.44 ± 0.07	0.15 ± 0.44 ± 0.07
Charge Flips	0.014 ± 0.006 ± 0.003	- ± -	0.011 ± 0.005 ± 0.002	0.025 ± 0.008 ± 0.005
MC Pred	0.087 ± 0.010 ± 0.043	0.096 ± 0.010 ± 0.048	0.203 ± 0.014 ± 0.101	0.385 ± 0.020 ± 0.192
Total Pred	0.101 ± 0.501 ± 0.043	0.096 ± 0.315 ± 0.048	0.364 ± 0.438 ± 0.126	0.560 ± 0.438 ± 0.206
data	0	0	0	0

Table 19: Observed event yields in high-p_T (pT > 20/10) dileptons passing the *pMSSW/sneutrino* signal selections ($H_T > 320$ GeV, $\not{E}_T > 120$ GeV) compared to expectations from simulation alone, and from the data-driven methods. The *simulated backgrounds* contribution includes contributions from genuine same-sign lepton pairs (WZ, ZZ, leptons from same-sign W from single-, double-parton, and $t\bar{t}W$ production), as well as electrons from converted photons in $V\gamma$ production. Entries with zero contributing events are reported with an uncertainty corresponding to one event. This uncertainty is not added to the total MC contribution. Systematic uncertainties (the second uncertainty if present) are displayed only for the final combined type of background, no systematic uncertainty is added for estimates with zero entries. Systematic uncertainties are 100% correlated among the channels.